JOURNAL OF GEOPHYSICAL RESEARCH, VOL. 87, NO. A7, PAGES 5063–5080, JULY 1, 1982

Coupled Hydromagnetic Wave Excitation and Ion Acceleration Upstream of the Earth's Bow Shock

MARTIN A. LEE

Space Science Center, University of New Hampshire, Durham, New Hampshire 03824

A self-consistent theory is presented for the excitation of hydromagnetic waves and the acceleration of 'diffuse' ions upstream of the earth's bow shock in the quasi-equilibrium that results when the solar wind velocity and the interplanetary magnetic field are nearly parallel. For the waves the quasi-equilibrium results from a balance between excitation by the ions, which stream relative to the solar wind plasma, and convective loss to the magnetosheath. For the diffuse ions the quasi-equilibrium results from a balance between injection at the shock front, confinement to the foreshock by pitch angle scattering on the waves, acceleration by compression at the shock front, loss to the magnetosheath, loss due to escape upstream of the foreshock, and loss via diffusion perpendicular to the average magnetic field onto field lines that do not connect to the shock front. Diffusion equations describing the ion transport and wave kinetic equations describing the hydromagnetic wave transport are solved self-consistently to yield analytical expressions for the differential wave intensity spectrum as a function of frequency and distance from the bow shock z and for the ion omnidirectional distribution functions and anisotropies as functions of energy and z. In quantitative agreement with observations, the theory predicts (1) exponential ion spectra at the bow shock in energy per charge, (2) a decrease in intensity and hardening of the ion spectra with increasing z, (3) a 30-keV proton anisotropy parallel to z increasing from -0.28 at the bow shock to $+0.51$ as $z \rightarrow \infty$ (4) a linearly polarized wave intensity spectrum with a minimum at $\sim 6 \times 10^{-3}$ Hz and a maximum at $\sim 2\text{–}3 \times 10^{-2}$ Hz, (5) a decrease in the wave intensity spectrum with increasing z, (6) a total energy density in protons with energies >15 keV about eight times that in the hydromagnetic waves.

1. INTRODUCTION

One of the outstanding problems in solar-terrestrial physics is the structure of the earth's foreshock, that region upstream of, and magnetically connected to, the earth's bow shock. It is a region rich in particle and wave phenomena, all intrinsic to the structure of the collisionless bow shock.

Of primary importance among the foreshock constituents are the energetic ions (3–200 keV/charge) and hydromagnetic waves (5×10^{-3}–10^{-1} Hz as measured in the spacecraft frame) which, apart from the bulk motion of the solar wind, energetically dominate that portion of the foreshock accessible to the ions. The ions are generally observed either as a 'reflected' component (3–10 keV/charge), a collimated beam propagating along the interplanetary magnetic field away from the bow shock, or as a 'diffuse' component (3–200 keV/charge) a nearly isotropic distribution in the frame of the spacecraft. Occasionally the two components are observed together as an 'intermediate' ion distribution.

The intermediate ion distribution is always associated with transverse large-amplitude hydromagnetic waves that are predominantly noncompressive, left-hand circularly polarized in the spacecraft frame, and nearly monochromatic. Relative to the solar wind they propagate upstream only to be convected back toward the bow shock in the spacecraft frame. The diffuse ion distribution is also always observed in association with large-amplitude hydromagnetic waves. These waves, however, are more complex. They exhibit a broader frequency spectrum and substantial compression that leads to cresting and the formation of 'shocklets.' The waves are never observed either in association with the reflected component or unaccompanied by energetic ions.

Paper number 2A0543.
0148-0227/82/002A-0543$05.00

The hydromagnetic waves were first reported and discussed by *Greenstadt et al.* [1968] by using Vela 3A data and *Fairfield* [1969] by using Explorer 34 data. The reflected ions were first detected by *Asbridge et al.* [1968] based on Vela observations, and the diffuse ions by *Lin et al.* [1974] based on Imp 6 data, although the clear distinction between these two populations was first recognized by *Gosling et al.* [1978]. More recently the observational study of the upstream ions and hydromagnetic waves has been a major goal of the ISEE mission. The result has been extensive and detailed observations of their behavior. The more general results from the ISEE mission on upstream particles and waves, including electrons and plasma waves at higher frequencies, have been presented in a special issue of the *Journal of Geophysical Research* (*86*, 4317–4536, 1981).

Early theoretical work [*Sonnerup*, 1969] indicated that the reflected component could in principle be produced by reflecting solar wind ions at the shock front such that the interaction is elastic in that frame moving along the shock front in which the upstream solar wind velocity is parallel to the magnetic field. *Barnes* [1970] predicted that the reflected ions would excite hydromagnetic waves that are right-hand circularly polarized and propagate upstream in the frame of the solar wind as observed (the sense of circular polarization is opposite in the solar wind and spacecraft frames since the solar wind speed is greater than the wave phase speed).

The waves should disrupt the reflected component by scattering the ions in pitch angle and thereby create the diffuse component. Recent work, which we address momentarily, has established that the scattered ions may return to the bow shock and be further accelerated via compression between the upstream waves and the shock front or between the upstream waves and the downstream magnetosheath turbulence. The result is the shock acceleration of energetic ions confined to the foreshock by the same waves which they excite.

Thus the upstream energetic ions and hydromagnetic waves provide an excellent space laboratory to study shock acceleration, the development of hydromagnetic turbulence, and the quasilinear and nonlinear wave-particle interaction. The existence of the space laboratory and extensive measurements within it by the ISEE mission is fortunate in view of the established importance of wave-particle processes in accelerating energetic particles on the sun and in interplanetary space and their presumed importance in the origins of cosmic rays. A problem common to most theories of shock acceleration is the origin of the scattering upstream turbulence. The hydromagnetic waves upstream of the earth's bow shock offer convincing evidence, which may be evaluated quantitatively, that the required upstream turbulence can be excited by the accelerated particles themselves.

In spite of the astrophysical promise, excellent observations, and their obvious importance, theoretical efforts to date have not come to grips with the coupled behavior of upstream ions and hydromagnetic waves. *Barnes* [1970] and, more recently, *Fredericks* [1975], *Gary et al.* [1981], and *Sentman et al.* [1981*b*] have calculated instability rates of the hydromagnetic waves, given the observed ion distributions. Others have treated the ion transport and acceleration, given the spatial diffusion coefficients arising from particle scattering in the upstream waves. Under various ad hoc assumptions on the form of the diffusion coefficient for transport parallel to the magnetic field, *Terasawa* [1979, 1981], *Lee et al.* [1981], *Forman* [1981], and *Ellison* [1981] have all obtained results in agreement with the observations of the energy spectra and anisotropy of the diffuse component. *Eichler* [1981] found that the observed exponential form of the ion energy spectra near the bow shock could be explained independent of the form of the wave intensity spectrum by invoking diffusive transport normal to the magnetic field and lateral free-escape along field lines not connected to the bow shock. All of these calculations are linear and cannot address the coupled behavior of the ions and waves.

We present for the first time a theory, albeit simplified, for the coupled behavior of the hydromagnetic waves and diffuse ions in the quasi-equilibrium that results when the magnetic field is nearly parallel to the solar wind velocity. The mathematical method is based on a formalism developed by *Skilling* [1975], which was recognized to be important in the theory of shock acceleration by *Bell* [1978]. Diffuse ion transport is described by diffusion equations, wave transport is described by wave kinetic equations, and the diffusion coefficients and wave growth rates are determined by quasilinear theory. Diffusion theory, which includes information on only the first two moments of each ion phase-space distribution function, is sufficiently simple both to embrace the spatial dependence and nonlinear behavior intrinsic to the problem and to yield an analytical solution. In spite of its simplicity, the theory yields ion and wave spectra in agreement with the extensive ISEE observations. In most cases the agreement is quantitatively good.

In section 2 we review the observations of upstream ions and hydromagnetic waves that motivate the scenario and model described in section 3. In sections 4 and 5 we present the ion transport equations and wave kinetic equations, respectively, and their solutions. In section 6 we present a detailed comparison of the solutions with the observations. In section 7 we summarize the theory, bring attention to its limitations, and suggest further work. The appendix presents the basic results utilized from quasilinear theory.

2. SUMMARY OF OBSERVATIONS

In this section we briefly summarize the observations of the energetic ions and hydromagnetic waves upstream of the earth's bow shock. The most detailed measurements have been made by instruments aboard the ISEE 1 and ISEE 2 satellites, whose orbits extend ~8 R_E upstream of the bow shock, and ISEE 3 in orbit about the sun-earth libration point ~200 R_E upstream. We concentrate on those measurements and follow in most part the review by *Gosling et al.* [1979] and the paper by *Hoppe et al.* [1981].

The properties of the upstream ions have been thoroughly investigated [e.g., *Anderson*, 1979; *Ipavich et al.*, 1981*a*; *Paschmann et al.*, 1981; *Sentman et al.*, 1981*a*; *Eastman et al.*, 1981; *Bonifazi and Moreno*, 1981; *Sanderson et al.*, 1981*a*; *Stevens and van Rooijen*, 1981*a*]. They are of two types: (1) The 'reflected' (R) ions are highly anisotropic. In the frame of the solar wind they stream along the magnetic field away from the bow shock. (2) The 'diffuse' (D) ions are approximately isotropic in the frame of the spacecraft near the bow shock. The two populations seldom coexist, although occasionally ions of an 'intermediate' nature are observed [*Paschmann et al.*, 1979]. Each population has a number density ~1% that of the solar wind. The particles are observed only when the spacecraft is magnetically connected with the bow shock as first suggested by *Lin et al.* [1974]. The particle intensity measurements show a characteristic 'on-off' pattern as the magnetic field direction varies and the particle guiding center trajectory in the interplanetary magnetic and electric fields passing through the spacecraft alternately connects and disconnects with the shock front.

The reflected ions extend from solar wind energies up to several keV with a peak intensity generally at ~4–5 keV and a steep decay beyond [*Gosling et al.*, 1978]. Occasionally, however, the reflected ions are observed with energies as high as ~65 keV [*Scholer et al.*, 1981*a*]. They are generally observed in bursts ranging from 1 or 2 min duration to an hour.

The diffuse ions extend from solar wind energies up to 100–200 keV, also with a peak at about 4–5 keV. Beyond about 30 keV they exhibit differential intensity spectra that are exponential in energy [*Ipavich et al.*, 1979, 1981*a*]. They are observed to have approximately solar wind composition and are best organized in terms of energy per charge (E/Q)—that is, the composition is nearly independent of E/Q. In a survey of 33 diffuse ion events, *Ipavich et al.* [1981*a*] found the differential intensity ratio of helium to protons at a given E/Q to vary from 1% to 15% with a mean of ~7%. The exponential spectra exhibit a range of e folding values of E/Q from 15 keV/Q to 25 keV/Q. In contrast with the R population, the diffuse ions are generally observed to endure for hours with relatively constant intensity to within a factor of 2 or 3 and thus exhibit a 'plateau' in a plot of logarithmic intensity versus time. The approach to the 'plateau' following a disconnected configuration requires less time for 30 keV particles (~10 min) than for 100-keV particles (~50 min), which therefore show less pronounced 'plateaus' [*Ipavich et al.*, 1981*a*]. The typical energy density in diffuse protons with energies greater than 15 keV is 200 eV cm^{-3} [*Ipavich et al.*, 1981*b*].

The diffuse ions extend from the bow shock out to ~200

R_E where they are observed at ISEE 3 only occasionally due to the low probability of magnetic connection to the bow shock [*Scholer et al.*, 1980*b*; *Sanderson et al.*, 1981*a*]. They are also observed in the magnetosheath and often appear to be continuous in intensity across the bow shock [*Asbridge et al.*, 1978]. There are, however, also bow shock crossings during which the diffuse ion intensity changes abruptly [*Scholer et al.*, 1979]. An investigation of 33 proton events observed by ISEE 1 at 30 keV reveals an average spatial decay away from the bow shock upstream with an e folding decay length of ~7 R_E [*Ipavich et al.*, 1981*a*]. The intensity observed at ISEE 3 is expectedly lower than that observed in the vicinity of the bow shock. Ion intensities at 30(65) keV/Q are reduced by a factor 4–15 (1.6–5) so that the spectra are harder at ~200 R_E [*Scholer et al.*, 1981*b*]. But the ions observed at ISEE 3 at diffuse ion energies are no longer diffuse; they are observed to stream along the magnetic field away from the bow shock with a hemispherical distribution in solid angle [*Scholer et al.*, 1980*b*]. Similar behavior is also observed on IMP 8 at ~25 R_E [*Sanderson et al.*, 1981*c*].

In the spacecraft frame the anisotropy of 30 keV diffuse protons increases from a negative value ~ −0.25 at the bow shock (indicating a flux toward the earth) through zero at about 6 R_E. Beyond 6 R_E the anisotropy increases further (indicating a flux toward the sun) to the large positive values observed at ISEE 3 [*Ipavich et al.*, 1980].

The diffuse and intermediate ion distributions are always observed in association with large-amplitude ($|\delta\mathbf{B}| \sim |\mathbf{B}|$) hydromagnetic waves with frequencies in the spacecraft frame in the range 5×10^{-3}–10^{-1} Hz. The waves are never observed in the presence of the R component or unaccompanied by upstream ions. The waves have been discussed in a review by *Formisano* [1979].

In association with the intermediate ions the hydromagnetic waves are predominantly transverse, noncompressive, and nearly monochromatic with peak power at about 0.03 Hz. The wave vectors $\mathbf{k}$ are determined by a minimum variance analysis [*Hoppe et al.*, 1981] and generally lie within a cone of apex half angle 45° about the direction of the magnetic field. The field fluctuation magnitude $|\delta\mathbf{B}|$ is generally a few times larger than $\delta|\mathbf{B}|$ with larger compression for larger values of ϕ where $\cos\phi = \mathbf{k} \cdot \mathbf{B}(kB)^{-1}$ (M. M. Hoppe and C. T. Russell, private communication, 1981). The time delay between the detection of wave crests at ISEE 1 and ISEE 2 is consistent with their propagating at the Alfvén speed upstream with respect to the solar wind [*Hoppe et al.*, 1981]. The waves are observed to be predominantly left-hand circularly polarized in the spacecraft frame. Since they are convected back toward the bow shock by the solar wind, however, the waves are right-hand circularly polarized in the frame of the solar wind [*Fairfield*, 1969; *Hoppe et al.*, 1981].

In association with the diffuse ions the hydromagnetic waves are more complex. They are compressive, with large fluctuations in the magnetic field strength and the solar wind number density, and exhibit a broad frequency spectrum with peak power also at about 0.03 Hz. The wave fronts have crested, leading to the formation of 'shocklets' and contributing to the broad frequency spectrum. Here again, the observed time delays between wave crest arrivals at ISEE 1 and ISEE 2 are consistent with propagation at approximately the Alfvén speed upstream relative to the solar wind. The polarization of the 'shocklets' is typically linear, but both right- and left-handed rotations are also observed [*Hoppe et al.*, 1981]. Comparison of the wave intensities observed on ISEE 2 and IMP 8 for the same event indicate that the hydromagnetic waves attenuate with distance from the bow shock [*Hoppe et al.*, 1981]. Hydromagnetic wave activity is virtually absent at ISEE 3 at ~200 R_E from the bow shock. However, the waves were observed in association with one diffuse ion event of smaller anisotropy than usual when ISEE 3 was only 80 R_E from the bow shock [*Sanderson et al.*, 1981*b*].

Both the hydromagnetic waves and the upstream ions are correlated with the orientation of the interplanetary magnetic field. *Greenstadt* [1976] demonstrated that the waves are present only when the angle θ' between the field and the shock normal is less than about 45°. By virtue of their close association the correlation holds for the diffuse ions as well. Conversely, the R component is only present when $\theta' \gtrsim 45°$. However, *Scholer et al.* [1980*a*] argue that the more fundamental correlation for the ions and waves is with the angle θ between the field and the solar wind velocity, or equivalently, with the connection time of the field line with the bow shock. Observation of 60-keV (120 keV) protons requires $\theta \lesssim 40°$ ($\theta \lesssim 20°$). The correlation with θ' arises because the shock normal is nearly parallel to the solar wind velocity over the nose of the bow shock.

3. A Scenario and A Model

As discussed in part in the introduction, the observations described in section 2 can be accounted for by the following scenario:

When a field line first connects to the bow shock accelerated ions stream upstream to create the reflected (R) component either by direct reflection of solar wind ions at the shock front [*Hudson*, 1965; *Sonnerup*, 1969] or by leakage from the downstream 'shock-heated' solar wind [*Ellison*, 1981; *Edmiston et al.*, 1982]. The observed energies of the R component are consistent with either the former [*Paschmann et al.*, 1980] or the latter [*Edmiston et al.*, 1982] acceleration process. Since the reflected ions stream upstream relative to the solar wind at a velocity necessarily greater than that of the solar wind $\mathbf{V}$, the beam is subject to the hydromagnetic streaming instability, the threshold of which is the Alfvén speed, V_A (≃ 0.1 V at 1 AU). The importance of this instability in the foreshock region was suggested by *Fairfield* [1969] and has been treated theoretically in this context by *Barnes* [1970], *Gary et al.* [1981], and *Sentman et al.* [1981*b*]. The same instability has been studied extensively for its potential role in limiting the anisotropy of galactic cosmic rays [*Lerche*, 1967; *Wentzel*, 1968; *Kulsrud and Pearce*, 1969; *Tademaru*, 1969; *Lee*, 1972; *Skilling*, 1975].

The result is the growth of hydromagnetic waves that propagate upstream and tend to be right-hand circularly polarized in the frame of the solar wind as observed in the presence of intermediate ion distributions that characterize this stage of the field line evolution [*Fairfield*, 1969; *Hoppe et al.*, 1981]. The growth of the waves is accompanied by scattering of the ions in pitch angle, driving the initially beamed ion distribution toward isotropy and reducing the wave growth rate. Since the scattering is approximately elastic in the frame of the solar wind, particles which are scattered back towards the bow shock gain considerable energy in the frame of the bow shock. They may again reflect from the shock front or the downstream magnetosheath

turbulence and again scatter in the upstream waves so that the process may be repeated. The resulting 'first-order Fermi acceleration' due to the compression of the solar wind at the bow shock and the coupling of the upstream ions to that compression via scattering and reflection at the shock front accelerates the R component into the diffuse (D) component. This general process is similar to that which occurs at interplanetary travelling shocks [*Fisk*, 1971] and at the forward and reverse shocks bounding corotating interaction regions in the solar wind [*Axford et al.*, 1977; *Fisk and Lee*, 1980].

Accordingly, as argued by *Bame et al.* [1980], the R component is the 'seed' population for the D component. Ions continue either to be reflected out of the solar wind at the bow shock or to escape from the downstream magnetosheath as the field line convects further along the shock front, but they are immediately scattered upstream of the shock front by the waves present and therefore not observed as a separate component in the presence of the diffuse ions. The diffuse ions are observed to be nearly isotropic in the spacecraft frame, which implies that they stream upstream relative to the solar wind at approximately the solar wind speed. They continue, therefore, to excite hydromagnetic waves, which continue to scatter the ions and keep them confined near the shock for further acceleration and wave excitation. The diffuse ions and hydromagnetic waves therefore exhibit a symbiotic relationship, each dependent on the other for its existence.

As the field line convects off the nose of the bow shock (radius $\simeq 10\ R_E$) the acceleration process becomes less efficient for two reasons: (1) the compression at the bow shock decreases and (2) because $(\hat{n} \cdot \mathbf{B})/|\mathbf{B}| > (\hat{n} \cdot \mathbf{V})/V$, where $\hat{n}$ is the unit normal to the shock front and $\mathbf{B}$ is the ambient interplanetary magnetic field, ions reflected at the shock front out of the solar wind actually lose energy in the frame of the bow shock, thus lowering the energy of the seed population. Wave and particle activity then decreases.

The proposed evolution requires sufficient time to generate the waves and accelerate the ions up to the observed energies of $\gtrsim 100$ keV. If the angle θ between $\mathbf{B}$ and $\mathbf{V}$ is larger than about 50°, only the R component is observed. For $\theta \lesssim 45°$ the D component is observed exclusively, implying that the time required ($\sim 20\ R_E/V \tan\theta$) to generate the diffuse ions is roughly 5 min. Angles $\theta \lesssim 20°$ are required to observe diffuse ions at energies of ~ 120 keV [*Scholer et al.* 1980*a*] implying that acceleration to the highest energies requires roughly 14 min. The fact that more time is required to accelerate ions to higher energies evidently explains the inverse velocity dispersion observed [e.g., *Ipavich et al.*, 1981*a*] as a field line slowly rotates to smaller values of θ.

For $\theta \lesssim 20°$ a quasi-equilibrium can evidently develop. Ions are continually reflected out of the solar wind at the shock front or escape from the magnetosheath and are 'injected' into the foreshock region with a range of energies of about 4–5 keV/nucleon. The injection at low energy is balanced by ion losses at higher energies into the downstream magnetosheath, upstream beyond the foreshock region, and via scattering normal to $\mathbf{B}$ onto field lines that are not connected to the nose of the bow shock. Hydromagnetic waves are continually excited by the ions and propagate upstream in the solar wind but are convected back into the bow shock and lost to the magnetosheath. The conditions at the bow shock (e.g., compression) vary sufficiently slowly as the field line convects along the curved shock front that the accelerated particles remain in quasi-equilibrium with these conditions at each point. The subject of this paper is a theoretical description of the quasi-equilibrium, of which the observed 'plateaus' are evidently a manifestation.

The diffuse upstream ions, as their name implies, are adequately described by diffusion theory, which requires that the particle scattering mean free path be small in comparison with the spatial scalelength of the ion distributions. The hydromagnetic waves are described by wave kinetic equations. The wave-particle interaction is assumed to be adequately described by quasilinear theory with minor corrections.

The streaming instability favors the growth of hydromagnetic waves with wave vectors $\mathbf{k}$ within about 30° of $\mathbf{B}$ [*Tademaru*, 1969] as observed [*Hoppe et al.*, 1981]: The growth rate of the Alfvén mode (left-hand circularly polarized when $\mathbf{k}_{\|}\mathbf{B}$) decreases rapidly for $\theta \gtrsim 30°$. The growth rate of the magnetosonic mode (right-hand circularly polarized when $\mathbf{k}_{\|}\mathbf{B}$) is relatively insensitive to θ, but Landau damping increases with increasing θ. Accordingly, we take all waves to propagate parallel or antiparallel to $\mathbf{B}$. We thereby preclude addressing the compressive nature of the upstream hydromagnetic waves observed in association with the diffuse ions. However, the compressive nature of the waves appears to be due partially to their large amplitude and in any case not essential to their interaction with the upstream ions. This supposition is supported by the observation that the waves are noncompressive in association with the intermediate ion distribution, a state characteristic of a smaller connection time of the field line to the shock front before nonlinear effects have substantially modified the wave intensity spectrum.

4. The Diffuse Upstream Ion Transport Equation

Under the restriction that $V \lesssim v$, where v is particle speed, the ion transport equation relevant to the quasi-equilibrium outlined in section 3 is

$$\frac{\partial}{\partial z}\left(K_{\|\,s}\frac{\partial f_s}{\partial z}\right) + \nabla_\perp \cdot \mathsf{K}_{\perp\,s} \cdot \nabla_\perp f_s + V\frac{\partial f_s}{\partial z} = 0 \qquad (1)$$

where z is pathlength parallel or antiparallel to $\mathbf{B}$ measured upstream from the bow shock at $z = 0$, $f_s(x, y, z, v)$ is the omnidirectional distribution function of ion species s, $K_{\|\,s}$ is the spatial diffusion coefficient parallel to $\mathbf{B}$, $\mathsf{K}_{\perp,s}$ is the spatial diffusion tensor perpendicular to $\mathbf{B}$, and $\nabla_\perp \equiv \hat{e}_x\partial/\partial x + \hat{e}_y\partial/\partial y$. There are no derivatives with respect to momentum in (1) since the solar wind is divergenceless over the scale of the upstream ions. Technically, equation (1) applies in the frame in which the electric field vanishes: $\mathbf{V} \times \mathbf{B} = 0$. However, since we consider only the case in which $\mathbf{B}$ and $\mathbf{V}$ are nearly parallel in the frame of the bow shock (or spacecraft), the transformation speed between the two frames is much less than V and the distinction between the two frames is irrelevant. Equation (1) neglects statistical acceleration by the upstream waves that can occur when waves propagate in both directions along the field. That acceleration process is second order in V_A/v where V_A is the Alfvén speed defined by $V_A^2 = B^2/4\pi\Sigma_s m_s n_s$, and m_s and n_s are the mass and number density of solar wind species s. Since $V_A \simeq 0.1\ V$ in the solar wind at 1 AU and shock acceleration is first order in V/v, statistical acceleration should play a negligible role in accelerating upstream ions.

Perpendicular diffusion provides access of the upstream ions to field lines that do not connect to the bow shock along which the ions can rapidly escape. Such unconnected field lines provide a lateral 'free-escape' boundary, a point stressed by *Eichler* [1981]. For simplicity we consider a flux tube of circular cross section and radius a, the field lines on the surface of which afford free escape: $f_s(x^2 + y^2 = a^2) = 0$. Assuming cylindrical symmetry about the axial field line and neglecting the possible dependence of $K_{\perp s}$ on $r = (x^2 + y^2)^{1/2}$, $\nabla_\perp \cdot K_{\perp,s} \cdot \nabla_\perp f_s$ may be rewritten as $K_{\perp s} r^{-1}\partial/\partial r(r\partial f_s/\partial r)$. Neglecting also the dependence of $K_{\parallel,s}$ on r and following *Eichler* [1981], $f_s(r, z, v)$ may be expanded in eigenfunctions as $f_s(r, z, v) = \sum_{n=1}^{\infty} \phi_{s\,n}(z, v) J_0(\xi_n r a^{-1})$ for $r < a$, where $J_0(x)$ is the standard Bessel function and ξ_n is its nth zero. The appropriate superposition over n is determined by the r dependence of the injected particles at the shock. If we take that dependence to be proportional to $J_0(\xi_1 r a^{-1})$, only the $n = 1$ term contributes. For any r dependence of injected particles, however, it can be shown that the $n = 1$ term dominates away from the immediate vicinity of the shock front. Here we simply neglect terms $n \neq 1$, so that $\phi_{s\,1} = f_s(0, z, v)$. It is then sufficient to consider the solution at $r = 0$, $f_s = f_s(0, z, v)$, which satisfies

$$\frac{\partial}{\partial z}\left(K_{\parallel s}\frac{\partial f_s}{\partial z}\right) - K_{\perp s}(\xi_1/a)^2 f_s + V\frac{\partial f_s}{\partial z} = 0 \qquad (2)$$

where we note that $\xi_1 \simeq 2.4$.

The parallel diffusion coefficient is given in terms of the pitch-angle diffusion coefficient, D_μ, by [*Earl*, 1974]

$$K_\parallel = \frac{1}{4}v^2 \int_{-1}^{1} d\mu (1 - \mu^2)^2 D_\mu^{-1} \qquad (3)$$

where $\mu = v_z/v$. In the Appendix we outline the derivation via quasilinear theory of D_μ due to a (possibly unstable) spectrum of right-hand and left-hand circularly polarized Alfvén waves (equation (A.9) from the appendix):

$$D_\mu = \frac{\pi}{2}\frac{\Omega_s^2}{B^2}\frac{(1 - \mu^2)}{v|\mu|} I\left(k = \frac{\Omega_s}{v\mu}, z\right) \qquad (4)$$

where Ω_s ($= q_s B/m_s c$), q_s and m_s are the gyrofrequency, charge, and mass of species s. The differential wave intensity $I(k, z) = I_+(k, z) + I_-(k, z)$ gives the power per unit wave number k in the magnetic field fluctuations [$\langle \delta\mathbf{B} \cdot \delta\mathbf{B}\rangle = \int_{-\infty}^{\infty} dk\, I(k, z)$]. $I_+(k, z)$ is the intensity in waves propagating in the $\hat{e}_z$ direction with $k > 0$ ($k < 0$) corresponding to right-hand (left hand) circularly polarized waves for $B > 0$ and the reverse polarizations for $B < 0$. $I_-(k, z)$ is the intensity in waves propagating in the $-\hat{e}_z$ direction with $k > 0$ ($k < 0$) corresponding to left-hand (right hand) circularly polarized waves for $B > 0$ and the reverse polarizations for $B < 0$.

The upstream power spectral density observed in association with diffuse ions typically exhibits a weak peak at ~0.03 Hz accompanied by a broad shoulder from $4 \times 10^{-3} - 4 \times 10^{-2}$ Hz over which it varies by perhaps a factor of 3 [*Childers and Russell*, 1972]. Beyond 0.04 Hz the power spectral density decreases rapidly with frequency. For the upstream hydromagnetic waves the measured frequency is due almost entirely to the Doppler shift since $V_A \simeq 0.1\ V$; therefore $2\pi\nu \simeq V|k|$, where V is approximately parallel to $\mathbf{B}$ and ν is measured in Hertz. According to (4), then, 330-keV protons interact with waves with $\nu \gtrsim 4 \times 10^{-3}$ Hz and 3.3-keV protons interact with waves with $\nu \gtrsim 4 \times 10^{-2}$ Hz. Thus the frequency range $\nu \gtrsim 4 \times 10^{-3}$ Hz is relevant to diffuse ions and the range, $\nu \gtrsim 4 \times 10^{-2}$ Hz, is relevant to ions with small μ. Now according to (3), $K_\parallel$ is dominated by values of μ where $(1 - \mu^2)^2 D_\mu^{-1}$ is large. From (4) small values of $|\mu|$ would be expected to dominate the integral where $|k|$ is large and $I(k, z)$ is correspondingly small. However, small values of μ correspond to pitch angles near 90°, precisely where nonlinear corrections are required which add substantially to D_μ [*Völk*, 1973; *Jones et al*, 1973; *Goldstein*, 1976]. In lieu of more detailed information, we assume that the nonlinear correction to D_μ suppresses the contribution of the neighborhood about $\mu = 0$ to the integral in (3). Over the remaining domain of μ the observed shoulder in the wave intensity motivates the replacement of $I(\Omega_s/v\mu, z)$ by $I(\Omega_s|\mu|/v\mu, z)$ in order to evaluate the integral. Equation (3) then yields

$$K_{\parallel s} = \frac{B^2}{4\pi}\frac{v^3}{\Omega_s^2}[J(\Omega_s/v, z)]^{-1} \qquad (5)$$

$$J(\Omega_s/v, z) \equiv \left\{\frac{1}{2}\sum_{+\,-}[I(\pm\Omega_s/v, z)]^{-1}\right\}^{-1}$$

The form of the perpendicular spatial diffusion coefficient $K_{\perp s}$ within quasilinear theory is on less firm foundation because the usual mathematical assumption of cylindrical symmetry about $\mathbf{B}$ precludes a flux normal to $\mathbf{B}$ so that no information on $K_{\perp,s}$ is obtained. Nevertheless, $K_{\perp,s}$ can be obtained via the average squared deviations from an initial field line of an ensemble of particle trajectories [*Jokipii*, 1966, 1971]. That result is consistent with the heuristic form $K_\perp = \eta r_g^2/(\lambda v^{-1})$, where r_g ($= v\Omega^{-1}$) is the gyroradius for $\mu = 0$, λ is the scattering mean free path parallel to $\mathbf{B}$, and η is a constant of order 1. That is, a particle random walks normal to $\mathbf{B}$ with a step length of approximately one gyroradius for each reversal of direction along the average field. With $K_\parallel = \frac{1}{3}\lambda v$ we have $K_\perp = \eta v^4\Omega^{-2}(3K_\parallel)^{-1}$. According to *Jokipii* [1971], $K_\perp$ is proportional to the power in magnetic field fluctuations parallel to $\mathbf{B}$. If the magnetic fluctuations are isotropic, Jokipii obtains $\eta = (1/6)$. However, Jokipii uses a questionable formula for $K_\parallel$ that generally underestimates $K_\parallel$. Use of (3) for $K_\parallel$ therefore requires a larger value of η to obtain the same value of $K_\perp$. Conversely, since magnetic fluctuations parallel to $\mathbf{B}$ are observed to be somewhat smaller in amplitude (M. M. Hoppe, private communication, 1981) than those perpendicular to $\mathbf{B}$ (in our model, which assumes parallel propagation, all magnetic field fluctuations are normal to $\mathbf{B}$), a smaller value of η is required. In view of the obvious uncertainty we take $\eta = 1$ and appeal to observations in section 6 to argue that $\eta = 1$ is a reasonable choice. Accordingly, we take

$$K_{\perp s} = \frac{4\pi v}{3B^2} J(\Omega_s/v, z) \qquad (6)$$

Substituting (5) and (6) into (2) we obtain

$$\frac{\partial}{\partial z}\left(\frac{K_{\parallel,s}^{\,0}}{J}\frac{\partial f_s}{\partial z}\right) - K_{\perp\,s}^{\,0} J(\xi_1/a)^2 f_s + V\frac{\partial f_s}{\partial z} = 0 \qquad (7)$$

where $K_{\parallel,s}^{\,0} \equiv JK_{\parallel s}$ and $K_{\perp\,s}^{\,0} \equiv K_{\perp\,s}J^{-1}$. Dividing by J and defining the independent variable

$$\zeta(\Omega_s/v, z) = \int_0^z J(\Omega_s/v, z')dz' \qquad (8)$$

we obtain from (7)

$$K_{\parallel s}{}^0 \frac{\partial^2 f_s}{\partial \zeta^2} + V\frac{\partial f_s}{\partial \zeta} - K_{\perp s}{}^0(\xi_1/a)^2 f_s = 0 \qquad (9)$$

The appropriate boundary condition as $z \to \infty$ is that $f_s(z) \to 0$. Two distinct cases arise: (1) If $\zeta(\Omega_s/v, z \to \infty) \to \infty$, then the solution to (9) satisfying the boundary condition is $f_s = C_s(v)\ \exp\ [-V(2K_{\parallel,s}{}^0)^{-1}\ (1 + \psi_s)\zeta]$ where $\psi_s \equiv [1 + 4K_{\parallel,s}{}^0 K_{\perp,s}{}^0(\xi_1/a)^2 V^{-2}]^{1/2}$ and $C_s(v)$ is an arbitrary function of v. (2) if $\zeta(\Omega_s/v, z \to \infty) = \zeta^0(\Omega_s/v)$, then the corresponding solution is $f_s = D_s(v)\ \exp\ [-V(2K_{\parallel,s}{}^0)^{-1}\zeta]\ \sinh\ [V(2K_{\parallel s}{}^0)^{-1}\psi_s(\zeta^0 - \zeta)]$, where $D_s(v)$ is an arbitrary function of v.

The functions $C_s(v)$ and $D_s(v)$ are determined by the conditions at the shock front that (1) the omnidirectional distribution function be continuous and (2) the discontinuity in the component of the energetic ion streaming normal to the shock front equal the rate at which particles are injected at the front. If particles are injected with speed $v_s{}^0$ and diffusive transport in the turbulent magnetosheath is negligible, those conditions require that the upstream omnidirectional distribution satisfy at $z = 0$:

$$-\frac{K_{\parallel,s}{}^0}{J(\Omega_s/v,0)}\frac{\partial f_s}{\partial z} + \beta V v \frac{\partial f_s}{\partial v} = N_s\delta(v - v_s{}^0) \qquad (10)$$

where $\beta \equiv \frac{1}{3}\ (1 - \rho_u/\rho_d)$, ρ_u/ρ_d is the ratio of upstream to downstream plasma densities, and $4\pi(v_s{}^0)^2 N_s$ is the number of ions of species s injected per unit area per unit time at the shock front with speed $v_s{}^0$. Ions are, of course, 'injected' with a range of energies; since it will be shown that the diffuse ion spectra at higher energies are not dependent on $v_s{}^0$ except for overall normalization, however, the assumption of monoenergetic injection can be made with impunity. Employing condition (10) to evaluate $C_s(v)$ we obtain in case 1

$$f_s(v,\zeta) = N_s(\beta V v_s{}^0)^{-1}\exp\left\{-(2\beta)^{-1}\int_{v_s{}^0}^{v} dv'(v')^{-1}\right.$$
$$\left.\cdot\,[1 + \psi_s(v')]\right\}\cdot\exp\{-V(2K_{\parallel s}{}^0)^{-1}\,[1 + \psi_s(v)]\zeta\} \qquad (11)$$

Employing condition (10) to evaluate $D_s(v)$ we obtain in case 2

$$f_s(v,\zeta) = N_s(\beta V v_s{}^0)^{-1}$$
$$\cdot\exp\left\{-(2\beta)^{-1}\int_{v_s{}^0}^{v} dv'(v')^{-1}\,[\![1 + \psi_s(v')\coth\,[V(2K_{\parallel s}{}^0)^{-1}\right.$$
$$\left.\zeta^0\,\psi_s(v')]\!]\right\}\cdot\exp\,[-V(2K_{\parallel s}{}^0)^{-1}\zeta]\,\sinh\,[V(2K_{\parallel s}{}^0)^{-1}$$
$$\cdot(\zeta^0 - \zeta)\psi_s(v)]\,\{\sinh\,[V(2K_{\parallel s}{}^0)^{-1}\,\zeta^0\psi_s(v)]\}^{-1} \qquad (12)$$

Case 1 corresponds to infinite 'resistance' to the propagation of ions upstream. It should be noted that this case requires perpendicular diffusion to yield other than a power law dependence on v at the shock front. Case 2 corresponds to an upstream 'free-escape' boundary. If we neglect perpendicular diffusion ($\psi_s = 1$) and note that $(\zeta^0/K_{\parallel s}{}^0)$ equals $\int_0^\infty dz(K_{\parallel,s})^{-1}$ (or $L/K_{\parallel,s}$ where L is a 'free-escape' boundary), in this case the velocity dependence at the shock is given by

$$\exp\left\{-\beta^{-1}\int_{v_s{}^0}^{v} dv'(v')^{-1}\right.$$
$$\left.\cdot\left[1 - \exp\left(-V\int_0^\infty dz(K_{\parallel s})^{-1}\right)\right]^{-1}\right\}$$

the same result obtained by *Lee et al.* [1981] and *Forman* [1981].

Case 1 might at first seem artificial since it requires a nonzero wave intensity far upstream, upon which the upstream ion distribution near the bow shock should not depend. Conversely, case 1 is attractive because there clearly exists an interplanetary wave intensity far upstream that results in infinite 'resistance' unless it is restricted to satisfy either $I(\Omega_s/v) = 0$ or $I(-\Omega_s/v) = 0$.

Case 2 is attractive because the derived quantities should not depend on the distant interplanetary wave intensity. From a pragmatic viewpoint, however, case 2 is unattractive because it involves the arbitrary function $\zeta^0(\Omega_s/v)$, which dominates the form of the ion energy spectrum. The function $\zeta^0(\Omega_s/v)$ is not determined by the wave kinetic equation to be discussed in section 5. The wave kinetic equation introduces an arbitrary function in case 1. However, that function is conveniently the differential wave intensity at great distances from the bow shock, which can be identified with the interplanetary spectrum, and upon which the derived quantities do not depend sensitively.

Thus, case 1 accommodates the interplanetary wave intensity and, with that intensity specified, is fully determined. Our considered view is that case 1 better models the quasi-equilibrium of diffuse upstream ions. We proceed on that basis.

Since ψ_s is independent of the wave intensity, the omnidirectional distribution function at the shock $f_s(v, 0)$ follows immediately from equation (11):

$$f_s(v,0) = N_s(\beta V v_s{}^0)^{-1}$$
$$\cdot\exp\left\{-(2\beta)^{-1}\int_{v_s{}^0}^{v} dv'(v')^{-1}\right.$$
$$\left.\left[1 + \left(1 + \frac{4}{3}(v')^4\xi_1{}^2\Omega_s{}^{-2}a^{-2}V^{-2}\right)^{1/2}\right]\right\} \qquad (13)$$

The integral may be evaluated to yield

$$f_s(v,0) = N_s(\beta V v_s{}^0)^{-1}$$
$$\cdot\{[(1 + (v_s{}^0)^4 u_s{}^{-4})^{1/2} + 1][(1 + (v_s{}^0)^4 u_s{}^{-4})^{1/2} - 1]^{-1}\}^{-(8\beta)^{-1}}$$
$$\cdot(v/v_s{}^0)^{-(2\beta)^{-1}}\{[(1 + v^4 u_s{}^{-4})^{1/2} + 1]$$
$$\cdot[(1 + v^4 u_s{}^{-4})^{1/2} - 1]^{-1}\}^{(8\beta)^{-1}}$$
$$\cdot\exp\{(4\beta)^{-1}[(1 + (v_s{}^0)^4 u_s{}^{-4})^{1/2} - (1 + v^4 u_s{}^{-4})^{1/2}]\} \qquad (14)$$

where $u_s{}^4 = \frac{3}{4}\,\Omega_s{}^2 a^2 V^2 \xi_1{}^{-2}$. For $v \gtrsim u_s$ the final exponential factor in (14) determines the dominant behavior of $f_s(v, 0)$, which is $\exp[-(E_s q_s{}^{-1})\sigma^{-1}]$, where $E_s (= \frac{1}{2}\ m_s v^2)$ is ion kinetic energy and σ is a constant independent of particle species. Accordingly, for large v we expect ion spectra exponential in E_s/q_s with the same e folding value of E_s/q_s ($= \sigma$) for all ion species, as is observed [*Ipavich et al.*, 1979]. This explanation for the observed exponential ion spectra in

terms of the product, $(K_{\parallel s}K_{\perp s})$, has been given by *Eichler* [1981]. A more thorough comparison of equation (14) with observations is presented in section 6.

We now summarize section 4 briefly. The ion transport equations (1) have been solved to yield the ion omnidirectional distribution functions as functions of v and ζ (equation (11)). Although the distributions at the shock front are obtained immediately by setting $\zeta = 0$ (equation (14)), their dependence on z requires the differential wave intensities in order to evaluate $\zeta(z)$. Wave kinetic equations are presented and solved in the next section, section 5, to yield the wave intensities in terms of ζ. Finally, inversion yields $\zeta(z)$ and therefore the self-consistent ion omnidirectional distributions, $f_s(v, z)$, and differential wave intensities, $I_\pm(k, z)$.

5. The Kinetic Equations for the Differential Wave Intensities

The hydromagnetic wave growth or damping rate due to the streaming upstream ions is derived in the appendix and presented as equation (A6). The expression involves the derivative with respect to μ of the phase-space distribution function, $F_s(v, \mu)$, which must be related to the omnidirectional distribution function $f_s(v)$. By definition $f_s(v) = \frac{1}{2}\int_{-1}^{1} d\mu F_s(v, \mu)$. A condition for the validity of diffusion theory, which is supported by observations of the upstream ions within 10 R_E of the bow shock, is that the phase-space distribution function be nearly isotropic; the simplest assumption is then $F_s(v, \mu) \simeq f_s(v) + A_s(v)\mu$, whereby $\partial F_s/\partial\mu = A_s(v)$. Since within diffusion theory the differential flux, or streaming, parallel to $\hat{e}_z$ in the solar wind frame is $-K_{\parallel}\partial f/\partial z$, it then follows that $A_s(v) = -3v^{-1} K_{\parallel s}\, \partial f_s/\partial z$. With that substitution expression (A6) may be rewritten as

$$\gamma_\pm(k, z) = \mp \frac{6\pi^3}{|k|}\frac{V_A}{c^2}\sum_s \frac{q_s^2}{m_s}\int_{w_s} dv\, v\left(1 - \frac{\Omega_s^2}{k^2v^2}\right)K_{\parallel s}\frac{\partial f_s}{\partial z} \tag{15}$$

where w_s is the greater of v_s^0 and $|\Omega_s/k|$, we have assumed $\gamma^2 \ll \omega_0^2$, and $\gamma_+(\gamma_-)$ is the growth (decay) rate of waves propagating in the $\hat{e}_z(-\hat{e}_z)$ direction (note from (11) that $\partial f_s/\partial z < 0$).

In the quasi-equilibrium under consideration the differential wave intensities, $I_+(k, z)$ and $I_-(k, z)$, satisfy the wave kinetic equations

$$-(V \mp V_A)\frac{\partial I_\pm}{\partial z} = 2\gamma_\pm I_\pm \tag{16}$$

where we neglect induced emission or absorption or spontaneous emission due to other processes than the quasilinear wave-particle interaction with the upstream ions. We note that $\gamma_\pm$ as presented in (15) is independent of the sign of k. Let $I_\pm^0(k)$ be the interplanetary wave intensity spectrum [lim $(z \to \infty)I_\pm(k, z) = I_\pm^0(k)$]. If $I_\pm^0(k) = I_\pm^0(-k)$, implying no net polarization of the interplanetary spectrum, then $I_\pm(k, z) = I_\pm(-k, z)$ and, from (5), $I(\Omega_s/v, z) = I(\Omega_s/v, z)$.

Neglecting V_A compared with V, using $\zeta(k, z)$ as independent variable, and noting from (15) that $\gamma_- = -\gamma_+ \equiv -\gamma$, (16) becomes

$$\frac{\partial I_\pm}{\partial\zeta} = \mp\frac{2\gamma}{V}\frac{I_\pm}{I_+ + I_-} \tag{17}$$

A first integral yields

$$I_+(k, z)I_-(k, z) = I_+^0(k)I_-^0(k) \tag{18}$$

The difference of (17) yields

$$\frac{\partial}{\partial\zeta}(I_+ - I_-) = -\frac{2\gamma}{V} \tag{19}$$

In general, equations (8), (11), (15), (18), and (19) combine to give integro-differential equations equations for $I_\pm(k, z)$. In order to approximate (15) for γ and simplify the calculation we note, if $K_{\parallel s}\partial f_s/\partial z$ $(= K_{\parallel s}^0\partial f_s/\partial\zeta)$ is a rapidly decreasing function of increasing v and $|k| < k_s^0 \equiv |\Omega_s|/v_s^0$, then the integral in (15) is controlled by $K_{\parallel s}\partial f_s/\partial z$ evaluated at the lower limit of integration, $w_s = |\Omega_s/k|$. The integral should then be equal to the product of $K_{\parallel s}\partial f_s/\partial z$ evaluated at $v = |\Omega_s/k|$ and a proportionality factor that should not depend sensitively on $f_s(v, z)$. For the explicit purpose of estimating the proportionality factor we utilize from (14) the asymptotic form of $f_s(v, \zeta = 0)$ $[\sim v^{2-(2\beta)^{-1}}\exp(-(4\beta)^{-1}u_s^{-2}v^2)]$ valid for large v $(\gtrsim u_s)$. Then

$$\gamma \sim -\sum_s \frac{6\pi^3 V_A q_s^2\Omega_s^2}{|k|c^2m_sk^2}\left(K_{\parallel s}\frac{\partial f_s}{\partial z}\right)_{v=|\Omega_s/k|}\int_1^\infty dx\, x^{3-(2\beta)^{-1}}(1 - x^{-2})e^{-\phi_s(x^2-1)} \tag{20}$$

where $\phi_s \equiv (4\beta)^{-1}u_s^{-2}(\Omega_s/k)^2$. Equation (20) is valid for $v \gtrsim u_s$, corresponding to $|k| \lesssim |\Omega_s|/u_s$. The integral in (20) equals $\frac{1}{2}e^{\phi_s}\phi_s^{-2+(4\beta)^{-1}}\{\Gamma[2 - (4\beta)^{-1}, \phi_s] - \phi_s\Gamma[1 - (4\beta)^{-1}, \phi_s]\}$ where $\Gamma(\alpha, \beta)$ is the incomplete gamma function. To be consistent with the previous asymptotic expansion of $f_s(v, 0)$ we replace the gamma functions by their asymptotic expansions in ϕ_s and obtain

$$\gamma \sim -\sum_s \frac{3\pi^3 V_A q_s^2\Omega_s^2}{|k|c^2m_sk^2}\left(K_{\parallel s}^0\frac{\partial f_s}{\partial\zeta}\right)_{v=|\Omega_s/k|}\phi_s^{-2}[1 - (2\beta)^{-1}\phi_s^{-1} + \quad] \tag{21}$$

Retaining only the leading term we have

$$\gamma \sim -\frac{1}{2}V\sum_s \alpha_s(k)(\partial f_s/\partial\zeta)_{v=|\Omega_s/k|}$$

$$\alpha_s(k) \equiv (4\beta)^2u_s^4\frac{6\pi^3V_Aq_s^2|k|}{Vc^2m_s\Omega_s^2}(K_{\parallel s}^0)_{v=|\Omega_s/k|} \tag{22}$$

where $f_s(v, \zeta)$ is known from (11).

Now substituting (22) into (19) we obtain upon integration

$$I_+(k, z) - I_-(k, z) = \sum_s \alpha_s(k)f_s(|\Omega_s/k|, z) + I_+^0(k) - I_-^0(k) \tag{23}$$

where we have noted that $f_s(v, z) \to 0$ as $z \to \infty$. Equations (18) and (23) have solutions

$$I_\pm = \frac{1}{2}\left\{\pm\left(\sum_s \alpha_s f_s - I_-^0 + I_+^0\right) + \left[\left(\sum_s \alpha_s f_s - I_-^0 + I_+^0\right)^2 + 4I_-^0 I_+^0\right]^{1/2}\right\} \tag{24}$$

Interplanetary magnetic field fluctuations in the frequency range 10^{-5}–10^{-3} Hz in the spacecraft frame consist predominantly of Alfvén waves propagating away from the sun and contributions from neighboring 'flux tubes' (with different magnetic field strengths but in pressure equilibrium) being convected past the observing spacecraft [*Belcher and Davis*, 1971; *Goldstein and Siscoe*, 1972]. The latter do not significantly affect energetic particles if flux tubes have greater lateral dimensions than the particle gyroradius. If we assume that the scattering interplanetary fluctuations in the frequency range relevant to diffuse upstream ion propagation (10^{-3}–10^{-1} Hz) are also predominantly Alfvén waves propagating away from the sun, then $I_-^0(k)$ should describe their differential intensity and $I_+^0(k)$ should be approximately zero. Taking $I_+^0(k) \simeq 0$, equation (24) yields

$$\begin{aligned} &\sum_s \alpha_s f_s > I_-^0 \quad I_+ \simeq \sum_s \alpha_s f_s - I_-^0 \\ &\qquad\qquad I_- \simeq 0 \\ &\sum_s \alpha_s f_s < I_-^0 \; I_+ \simeq 0 \\ &\qquad\qquad I_- \simeq I_-^0 - \sum_s \alpha_s f_s \end{aligned} \tag{25}$$

In either case given in (25)

$$\left(\sum_s \alpha_s f_s \gtrless I_-^0\right), \; I_+ + I_- = \left|\sum_s \alpha_s f_s - I_-^0\right|$$

We note that f_s is known as a function of ζ (see equation (11)) and $\partial\zeta/\partial z = I_+ + I_-$ so that

$$z = \int_0^\zeta d\zeta' \left|\sum_s \alpha_s f_s - I_-^0\right|^{-1} \tag{26}$$

Waves of a given wave number k are resonant with ions of species s with speed $v = |\Omega_s/k|$ or with energy per charge E_s/Q_s (where $Q_s = q_s/q_p$) $= \frac{1}{2} m_s Q_s^{-1}(\Omega_s/k)^2 \propto \Omega_s$. Since the ion differential intensity spectra are observed to be exponential in E/Q, helium, with $\Omega_{He} = \frac{1}{2}\Omega_p$, will therefore dominate protons in determining the wave spectrum at small k in (23). The species with $q_s \geq 3q_p$ are negligible in expressions (23)–(26) in comparison with helium since $\Omega_s \sim \Omega_{He}$ and together they have a differential intensity about 8% that of helium [*Ipavich et al.*, 1981*a*].

We note from (11) that $f_s(v, \zeta) = f_s(v, 0)\exp(-\lambda_s\zeta)|_{v=|\Omega_s/k|}$, where $\lambda_s \propto \Omega_s^{-1}\,[1 + (1 + \Omega_s^4 k^{-4} u_s^{-4})^{1/2}]$ and the constant of proportionality is independent of species. It will be demonstrated in section 6 that helium and protons contribute equally to expressions (23)–(26) at the bow shock at a frequency ($\sim 1.1 \times 10^{-2}$ Hz) corresponding to approximately 44-keV protons and 22-keV/Q helium, for which $\Omega_p^4 k^{-4} u_p^{-4}$ is approximately 4. Protons dominate at higher frequencies corresponding to lower energies; helium dominates at lower frequencies corresponding to higher energies. Therefore, where helium contributes substantially to (26), $\lambda_{He} \sim \lambda_p$. Furthermore, for any k, $\lambda_{He} > \lambda_p$ so that the contribution of helium relative to protons decreases with distance from the bow shock. Accordingly we take $\lambda_{He} = \lambda_p$ in expression (26), which may be evaluated to yield

$$\begin{aligned} f_p(v, z) = f_p(v, 0)\, &I_-^0(\Omega_p/v)\{\alpha_p(\Omega_p/v) f_p(v, 0) \\ &+ \alpha_{He}(\Omega_p/v) f_{He}(v\Omega_{He}/\Omega_p, 0) \\ &- [\alpha_p(\Omega_p/v) f_p(v, 0) \\ &+ \alpha_{He}(\Omega_p/v) f_{He}(v\Omega_{He}/\Omega_p, 0) - I_-^0(\Omega_p/v)] \\ &\exp\,[\mp V(2K_{\parallel p}{}^0)^{-1}(1 + \psi_p) I_-^0(\Omega_p/v)\, z]\}^{-1} \end{aligned} \tag{27}$$

where $f_p(v, 0)$ and $f_{He}(v, 0)$ are given by (14) and the ($\pm$) sign refers to $\Sigma_s \alpha_s(k) f_s(|\Omega_s/k|, z) \gtrless I_-^0(k)$. From (27) it is clear that, for a given k, $\Sigma_s \alpha_s(k) f_s(|\Omega_s/k|, z)$ is either greater than $I_-^0(k)$ for all z or less than $I_-^0(k)$ for all z.

In (27) it should be noted that, for $\Sigma_s \alpha_s f_s > I_-^0$,

$$\begin{aligned} f_p(v, z) \to f_p(v, 0) I_-^0(\Omega_p/v)\{&\alpha_p(\Omega_p/v) f_p(v, 0) \\ &+ \alpha_{He}(\Omega_p/v) f_{He}(v\Omega_{He}/\Omega_p, 0)\}^{-1} \end{aligned}$$

as $z \to \infty$ in apparent contradiction with the boundary condition stated in section 4 that $f_p \to 0$ as $z \to \infty$. There is no contradiction as long as $I_+^0(k)$ is not identically zero. Where $\Sigma_s \alpha_s f_s = I_-^0$, $I = 0(I_+^0)$ so that $\partial\zeta/\partial z \simeq 0(I_+^0)$ and a large range of z corresponds to a very small range of ζ. That large range extends to $z \to \infty$ as $I_+^0 \to 0$. Interestingly, this minimum in $I(k)$ yields ion solutions that appear as free-streaming solutions with finite 'resistance,' an option with attractive features and observational support that, however, was discarded in section 4 since it involved an essential unknown function of k. Here we adopt (27) under the assumption that $I_+^0(k)$ is sufficiently small that the expression holds for values of $z(<200\, R_E)$ where measurements are made.

For $\Sigma_s \alpha_s f_s \gtrless I_-^0$ we obtain from (25) and (27) (taking $\lambda_{He} = \lambda_p$)

$$\begin{aligned} I_\pm(k, z) = I_-^0(k)&|\alpha_p(k) f_p(|\Omega_p/k|, 0) \\ &+ \alpha_{He}(k) f_{He}(|\Omega_{He}/k|, 0) - I_-^0(k)| \\ &\{I_-^0(k) + [\alpha_p(k) f_p(|\Omega_p/k|, 0) + \alpha_{He}(k) f_{He}(|\Omega_{He}/k|, 0)] \\ &[\exp[\pm \tfrac{1}{2} V(K_{\parallel p}{}^0)^{-1}(1 + \psi_p))_{v=|\Omega_p/k|}\, I_-^0(k) z] - 1]\}^{-1} \end{aligned} \tag{28}$$

As in (27) we assume that $I_+^0(k)$ is sufficiently small that equation (28) is valid for values of $z < 200\, R_E$.

If $|k| > |\Omega_s|/v_s^0$, γ is dominated by protons and we obtain from (15)

$$\gamma = \frac{3\pi^3 V V_A q_p^2}{|k| c^2 m_p}\left(M_1 - \frac{\Omega_p^2}{k^2} M_2\right)$$

$$(M_1, M_2) = \int_{v_p{}^0}^\infty dv\, v(1, v^{-2})[1 + \psi_p(v)] f_p(v, z) \tag{29}$$

where $f_p(v, z)$ is given by (27). It is clear from the general expression (15) that $M_1 > \Omega_p{}^2 k^{-2} M_2$. In general, the extra factor v^{-2} in M_2 results in M_2 contributing substantially less than M_1 to γ, so that M_2 can be neglected for illustrative purposes. Neglecting V_A compared with V, equation (16) yields solutions for $|k| > |\Omega_p|/v_p{}^0$

$$I_\pm(k, z) = I_\pm^0(k)\exp\left[\pm 2V^{-1}\int_z^\infty dz'\, \gamma(k, z')\right] \tag{30}$$

Since $I_+^0(k)$ is small and $\gamma \propto |k|^{-1}$, $I(k)$ $(= I_+(k) + I_-(k))$ will drop precipitously for $|k| \gtrsim |\Omega_p|/v_p{}^0$ and then recover to $I_-^0(k)$ for larger $|k|$.

From (11), (14), and (27) we readily infer the omnidirec-

tional distribution functions of helium and the other minor ions:

$$
\begin{aligned}
{}_{s}(v, z) = {} & f_s(v, 0)\,[I_-^0(\Omega_s/v)]^{\sigma} \\
& \cdot \{\alpha_p(\Omega_s/v) f_p(A_s Q_s^{-1} v, 0) \\
& + \alpha_{\mathrm{He}}(\Omega_s/v) f_{\mathrm{He}}(\tfrac{1}{2} A_s Q_s^{-1} v, 0) \\
& - [\alpha_p(\Omega_s/v) f_p(A_s Q_s^{-1} v, 0) \\
& + \alpha_{\mathrm{He}}(\Omega_s/v) f_{\mathrm{He}}(\tfrac{1}{2} A_s Q_s^{-1} v, 0) - I_-^0(\Omega_s/v)] \\
& \cdot \exp\{\mp V(2K_{\parallel,s}{}^0)^{-1}[Q_s A_s^{-1} \\
& + (Q_s^2 A_s^{-2} + E_s^2 Q_s^{-2} E_0^{-2})^{1/2}] I_-^0(\Omega_s/v) z\}^{-\sigma}
\end{aligned}
\tag{31}
$$

where

$$
\begin{aligned}
\sigma = {} & [1 + (1 + E_s^2 Q_s^{-2} E_0^{-2})^{1/2}][Q_s A_s^{-1} \\
& + (Q_s^2 A_s^{-2} + E_s^2 Q_s^{-2} E_0^{-2})^{1/2}]^{-1}
\end{aligned}
$$

and where $A_s \equiv m_s/m_p$, $E_0 \equiv \frac{1}{4} 3^{1/2} a V \xi_1^{-1} q_p |B| c^{-1}$, and $(\pm)$ refers to $\alpha_p(\Omega_s/v) f_p(A_s Q_s^{-1} v, 0) + \alpha_{\mathrm{He}}(\Omega_s/v) f_{\mathrm{He}}(\frac{1}{2} A_s Q_s^{-1} v, 0) - I_-^0(\Omega_s/v) \gtrless 0$.

6. Comparison With Observations

We now compare the theoretical results derived in section 5 with the observations outlined in section 2. As representative solar wind parameters we take $V = 400$ km s^{-1}, $V_A = 40$ km s^{-1}, and $B = 5 \times 10^{-5}$ G. For the compression at the bow shock we take the observed average value of $\simeq 3.4$ [*Argo et al.*, 1967], implying $\beta = 0.235$. For the typical lateral distance to unconnected field lines a, we take the characteristic dimension of the nose of the bow shock ($\simeq 10\ R_E$). Since the reflected component, which peaks at about 5 keV/nucleon, is the 'seed' population for the diffuse ions we take $v_s^0 = 980$ km s^{-1}. In order to normalize $f_p(v, z)$ (determine N_p), we take $f_p(2.4 \times 10^3$ km s^{-1}, $z = 0)$ from observations of 30-keV protons: in a statistical survey of 33 diffuse proton events *Ipavich et al.* [1981*a*] give as a characteristic differential intensity at the bow shock 4×10^3 protons (cm^2 s sr keV)$^{-1}$, which is equivalent to $f_p = 7.3 \times 10^{-29}$ protons cm^{-6} s^3. In order to normalize $f_{\mathrm{He}}(v, z)$ (determine N_{He}), we take $f_{\mathrm{He}}(1.7 \times 10^3$ km s^{-1}, $z = 0)$ from observations of 30 keV/Q helium; in the same survey, *Ipavich et al.* [1981*a*] determine the average differential intensity ratio of helium to protons at 30 keV/Q to be 7%, implying a differential intensity of 2.8×10^2 alpha particles (cm^2 s sr keV/Q)$^{-1}$, which is equivalent to $f_{\mathrm{He}} = 2.0 \times 10^{-29}$ alpha particles cm^{-6} s^3. From *Russell* [1972] we take the characteristic power spectrum of the radial component of the interplanetary magnetic field during quiet periods as $3.3 \times 10^{-2}(0.1/\nu)^{3/2}$ in units of γ^2/Hz, where ν is the fluctuation frequency in the spacecraft frame in units of Hertz. Multiplying by a factor of 3 to include all three components under the assumption of isotropy, we have $\mathscr{E}(\nu) = 0.1\ (0.1/\nu)^{3/2} \gamma^2$/Hz, which is equivalent to $I_-^0(k) = 3.2 \times 10^{-5}(1.57 \times 10^{-8}/k)^{3/2}$ G^2 cm, where $2\pi\nu \simeq kV$ (under the assumptions $V_A \ll V$ and $\mathbf{v} \cdot \mathbf{B} = VB$).

Equation (14) for the ion omnidirectional distribution function at the shock front may be written in terms of ion energy E_s and proton-normalized charge $Q_s (= q_s/q_p)$ as

$$
\begin{aligned}
f_s(E_s, 0) = {} & C_s (E_s/Q_s)^{-(4\beta)^{-1}} \{[[1 + (E_s/Q_s)^2 E_0^{-2}]^{1/2} + 1] \\
& \cdot [[1 + (E_s/Q_s)^2 E_0^{-2}]^{1/2} - 1]^{-1}\}^{(8\beta)^{-1}} \\
& \cdot \exp\{-(4\beta)^{-1}[1 + (E_s/Q_s)^2 E_0^{-2}]^{1/2}\}
\end{aligned}
\tag{32}
$$

where C_s is a constant dependent on species, and $E_0 (= \frac{1}{4} 3^{1/2} a V \xi_1^{-1} q_p |B| c^{-1})$ is independent of species. Except for overall normalization, all ion species have the same energy spectrum as a function of E_s/Q_s at the bow shock in agreement with observations at ISEE 1, which is generally located close to the bow shock [*Ipavich et al.*, 1979]. E_0 has the value of 23 keV for our choice of parameters. For energies $E_s/Q_s \gtrsim E_0$ the dominant behavior of each ion spectrum is exponential in E_s/Q_s with an e folding value equal to $4\beta E_0 \simeq 21.6$ keV, again in agreement with observations [*Ipavich et al.*, 1979]. The observed range of the e folding energy per charge (15–25 keV) is readily explained by a range of values of a (6.9–11.6 R_E, respectively), depending on the particular geometry of the quasi-equilibrium. *Ipavich et al.* [1979] actually determine the exponential dependence between 30 keV/Q and 120 keV/Q in terms of the differential intensity $\mathscr{J}(E)$, which is proportional to $E_s f_s(E_s)$. Immediately following, in a detailed discussion of the proton spectrum, we show that the differential intensity between 30 and 120 keV/Q predicted by equation (31) at the bow shock is indistinguishable from exponential. The exponential behavior at the bow shock, which arises from the fact that $K_{\perp,s} K_{\parallel,s} \propto (E_s/Q_s)^2$, independent of the wave intensity, was first explained in this way by *Eichler* [1981] by using a linear theory. It should be noted from (31), however, that the simple dependence of the ion distribution functions on E_s/Q_s described by (32) holds only at the shock front.

We now consider the proton spectrum described by (27). In Figure 1 we plot the predicted proton differential intensity spectrum for several values of z given in units of earth radii (R_E). The dashed portion of each curve indicates that range of E for which the assumption that $K_{\parallel,p} \partial f_p/\partial z$ is a rapidly decreasing function of increasing v (or E) is not satisfied, an assumption on which the approximation of γ leading to (22) is formally based. Nevertheless, the dashed portions should indicate qualitatively the correct behavior. The spectrum at $z = 0$ shows that $\mathscr{J}(E, 0)$ is indistinguishable from its asymptotic leading behavior [$\mathscr{J}(E) \sim \exp(-E/21.6$ keV)] for $E \gtrsim 30$ keV. Since ions cannot lose energy, there are no protons with $v < v_p^0$ so that the spectra are 'donut' distributions as observed [*Paschmann et al.*, 1981]. The critical behavior at $E = E_c \simeq 125$ keV arises from the fact that the wave intensity at the corresponding wave number ($k = \Omega_p/v$) is approximately zero as discussed briefly in section 5 (see equation (25)). For $E < E_c$ the spectra harden with increasing z in agreement with observations at ISEE 3 [*Scholer et al.*, 1981*b*].

For $V(2K_{\parallel,p}{}^0)^{-1}(1 + \psi_p) I_-^0(\Omega_p/v) z \lesssim 1$, the exponential in equation (27) may be expanded to yield

$$
\begin{aligned}
f_p(v, z) & \simeq f_p(v, 0)[1 + z L^{-1}(v)]^{-1} \\
L^{-1}(v) & \equiv V(2K_{\parallel,p}{}^0)^{-1}(1 + \psi_p) |\alpha_p(\Omega_p/v) f_p(v, 0) \\
& \quad + \alpha_{\mathrm{He}}(\Omega_p/v) f_{\mathrm{He}}(v\Omega_{\mathrm{He}}/\Omega_p, 0) - I_-^0(\Omega_p/v)|
\end{aligned}
\tag{33}
$$

where $L(v)$ is the characteristic scale length for the decrease in particle intensity away from the bow shock. $L(v)$ increases rapidly with increasing v until $E = E_c$ where it is singular;

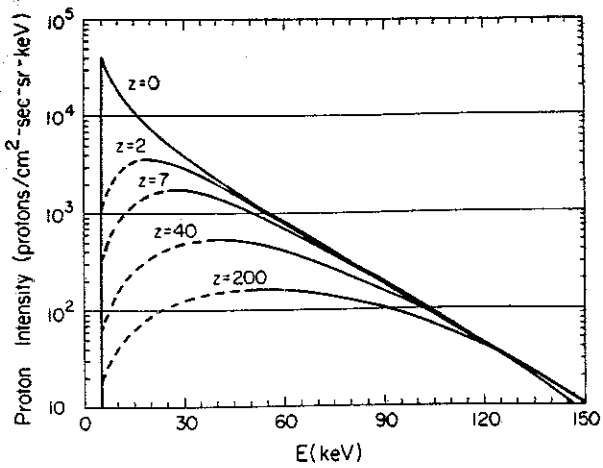

Fig. 1. The predicted proton differential intensities at several distances from the bow shock in units of R_E. The intensity of 30 keV protons at the bow shock is taken to be 4×10^3 protons (cm^2 s sr keV)$^{-1}$ [*Ipavich et al.*, 1981*a*]. The dashed portion of each curve indicates that range of energy for which the assumption that $K_{\parallel,s}\partial f_s/\partial z$ is a rapidly decreasing function of increasing energy is not satisfied.

thereafter $L(v)$ decreases with increasing v. $L(30\text{ keV}) \simeq 5.3\ R_E$ in good agreement with the average observed e folding scalelength of about $7R_E$ determined by *Ipavich et al.* [1981*a*] from 33 diffuse proton events at 30 keV.

From (27) for large z we obtain the limiting spectrum

$$f_p(v, z \to \infty) = I_-^0(\Omega_p/v) f_p(v, 0)\{\alpha_p(\Omega_p/v) f_p(v, 0) + \alpha_{He}(\Omega_p/v) f_{He}(v\Omega_{He}/\Omega_p, 0)\}^{-1} \qquad E < E_c \qquad (34)$$

$$f_p(v, z \to \infty) \simeq 0 \qquad E > E_c$$

Again, the singular behavior here is partially due to the working hypothesis that $I_+^0(k) \to 0$ as discussed in section 5. For small but finite $I_+^0(k)$, $f_p(v, z)$ exhibits the behavior described in (34) (which, as we shall see, corresponds to free streaming) for a large range in z before eventually decreasing exponentially for larger z.

In Figure 2 we plot the predicted helium differential intensity as a function of energy per charge ($E/2$) for the same values of z chosen in Figure 1. The dashed portions of the curves indicate the same quantitative limitation of the theory discussed with reference to Figure 1. The proton and helium spectra are identical in form at the bow shock as a result of their dependence on E_s/Q_s only at $z = 0$, but exhibit a more complex dependence for $z \neq 0$.

In Figure 3 we plot the predicted proton differential intensity as a function of z for 30 keV protons (solid curve). For comparison we include the data of *Ipavich et al.* [1981*a*]; the points give the observed intensity at 30 keV and the inferred distance to the bow shock for each of 33 diffuse proton events. The scatter presumably results from the various geometries and range of parameters in the sample; nevertheless the predicted behavior reproduces the observed trend. Also shown are the predicted differential intensities of 60-keV protons (dashed curve) and 30 keV/Q helium (dash-dot curve) as functions of z.

Ion anisotropy, $\xi_s(v, z)$, is given in terms of the ion streaming parallel to $\hat{e}_z(S_s = -K_{\parallel,s}\partial f_s/\partial z + \frac{1}{3}Vv\partial f_s/\partial v)$ by $\xi_s = 3S_s(vf_s)^{-1}$ if $|\xi_s| \lesssim 0.3$ [*Gleeson and Axford*, 1967]. From (27) [$\Sigma_s \alpha_s f_s > I_-^0$ or $E < E_c$] we obtain for protons

$$\begin{aligned} vV^{-1}\xi_p(v, z) = {} & \tfrac{3}{2} + (\tfrac{3}{2} - (2\beta)^{-1})(1 + \psi_p) \\ & - [\alpha_p(\Omega_p/v) f_p(v, 0) + \alpha_{He}(\Omega_p/v) f_{He}(v\Omega_{He}/\Omega_p, 0) \\ & + [I_-^0(\Omega_p/v) - \alpha_p(\Omega_p/v) f_p(v, 0) \\ & - \alpha_{He}(\Omega_p/v) f_{He}(v\Omega_{He}/\Omega_p, 0)] \\ & \cdot \exp[-V(2K_{\parallel,p}^0)^{-1}(1 + \psi_p) I_-^0(\Omega_p/v) z]]^{-1} \\ & \cdot \{[\alpha_p(\Omega_p/v) f_p(v, 0)[2 - (2\beta)^{-1}(1 + \psi_p)] \\ & + \alpha_{He}(\Omega_p/v) f_{He}(v\Omega_{He}/\Omega_p, 0) \\ & \cdot [2 - (2\beta)^{-1}(1 + (1 + \tfrac{1}{4}v^4 u_p^{-4})^{1/2})]] \\ & \cdot [[1 - \exp[-V(2K_{\parallel,p}^0)^{-1}(1 + \psi_p) I_-^0(\Omega_p/v) z]] \\ & + [[\tfrac{3}{2} I_-^0(\Omega_p/v) - V(2K_{\parallel,p}^0)^{-1}(1 + \psi_p) I_-^0(\Omega_p/v) z \\ & \cdot [I_-^0(\Omega_p/v) - \alpha_p(\Omega_p/v) f_p(v, 0) \\ & - \alpha_{He}(\Omega_p/v) f_{He}(v\Omega_{He}/\Omega_p, 0)] \\ & \cdot [-\tfrac{3}{2} + 2(E/E_0)^2 \psi_p^{-1}(1 + \psi_p)^{-1}]] \\ & \cdot \exp[-V(2K_{\parallel,p}^0)^{-1}(1 + \psi_p) I_-^0(\Omega_p/v) z]\} \end{aligned} \qquad (35)$$

Evaluating expression (35) at $z = 0$ we have $\xi_p(E < E_c, 0) = (V/v)(1 + \psi_p)[\frac{3}{2} - (2\beta)^{-1}]$, which equals -0.28 at 30 keV, indicating flow into the magnetosheath in quantitative agreement with the observed value of about -0.25 [*Ipavich et al.*, 1980]. It is also readily seen that

$$\begin{aligned} \xi_p(E < E_c, z \to \infty) = (V/v)\{1 + {} & \tfrac{3}{2}\psi_p \\ & + (2\beta)^{-1}\alpha_{He}(\Omega_p/v) f_{He}(v\Omega_{He}/\Omega_p, 0) \\ & \cdot [(1 + \tfrac{1}{4}v^4 u_p^{-4})^{1/2} - \psi_p][\alpha_p(\Omega_p/v) f_p(v, 0) \\ & + \alpha_{He}(\Omega_p/v) f_{He}(v\Omega_{He}/\Omega_p, 0)]^{-1}\} \end{aligned}$$

which equals 0.51 for 30-keV protons, indicating flow away from the bow shock. Although the calculated anisotropy as $z \to \infty$ is larger than that which can be accommodated with rigor within diffusion theory, it indicates rapid free streaming

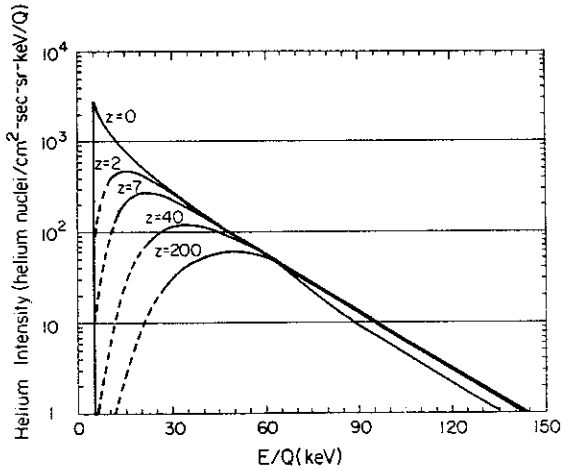

Fig. 2. The predicted helium differential intensities at several distances from the bow shock in units of R_E. The intensity of 30 keV/Q helium at the bow shock is taken to be 280 helium nuclei (cm^2 s sr keV/Q)$^{-1}$ [*Ipavich et al.*, 1981*a*]. The dashed portion of each curve indicates that range of energy per charge for which at the relevant ion energies $K_{\parallel,s}\partial f_s/\partial z$ is not a rapidly decreasing function of energy as assumed

of the particles away from the bow shock at large distances as observed. Although the presence of the interplanetary wave spectrum and the boundary condition $f_s(v, z \to \infty) \to 0$ precludes an anisotropy as $z \to \infty$, it is an interesting feature of the model that free-streaming behavior, as observed at ISEE 3, is exhibited for a large range of z due to the near absence of sunward propagating waves in the solar wind. Expression (31) yields similarly the helium anisotropy, which exhibits analogous behavior. In Figure 4 we plot $\xi_p(v, z)$ for 30-keV protons (solid curve) and 60-keV protons (dashed curve) and $\xi_{He}(v, z)$ for 30-keV/Q helium (dash-dot curve) versus z in units of R_E. The reversal of the sign of $\xi_p(30\text{ keV}, z)$ at $z = 2.4\ R_E$ is in good agreement with results inferred from a sample of diffuse proton events [*Ipavich et al.*, 1980].

We now turn to the wave spectra. In Figure 5 we present the power spectral densities predicted from (28) for several values of z in units of R_E. The spectra, $\mathscr{E}(\nu)[=4\pi 10^{10} V^{-1} I_-^0(k)]$, are presented in units of γ^2/Hz as functions of ν in units of Hz ($2\pi\nu = kV$). As in Figure 1, the dashed portions of the curves indicate ranges of frequency where the corresponding ion distributions do not satisfy the assumed rapid decrease with increasing v required to derive the growth rate as given in (22). Nevertheless, the curves should qualitatively describe the spectra in those frequency ranges. The dotted lines indicate schematically the precipitous decrease in power beyond $\nu \simeq 3.1 \times 10^{-2}$ Hz described in section 5 following (30) and the gradual return to the interplanetary spectrum, all due to the absence of protons with energies less than 5 keV, that energy cyclotron resonant with 3.1×10^{-2} Hz if $|\mu| = 1$. The plus sign indicates ion-excited waves propagating away from the bow shock relative to the solar wind; the minus sign indicates partially damped interplanetary waves propagating toward the bow shock. As indicated in (25), the two directions of propagation do not coexist at a given frequency if $I_+^0(k) = 0$. The zero in the wave intensity at $\nu \simeq 6 \times 10^{-3}$ Hz, providing the transition between ion-excited and interplanetary waves, is the cause of the independence of the 125-keV proton intensity on z as

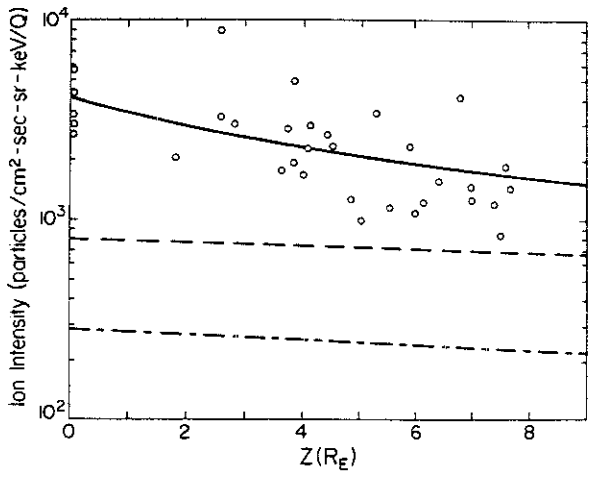

Fig. 3. The predicted differential intensities of 30-keV protons (solid curve), 60-keV protons (dashed curve), and 30-keV/Q helium (dash-dot curve) versus distance from the bow shock in units of R_E. Measurements of 33 diffuse proton events by the University of Maryland/Max Planck Institute experiment on ISEE 1 (taken from *Ipavich et al.* [1981*a*]) are shown for comparison with the 30-keV proton intensity

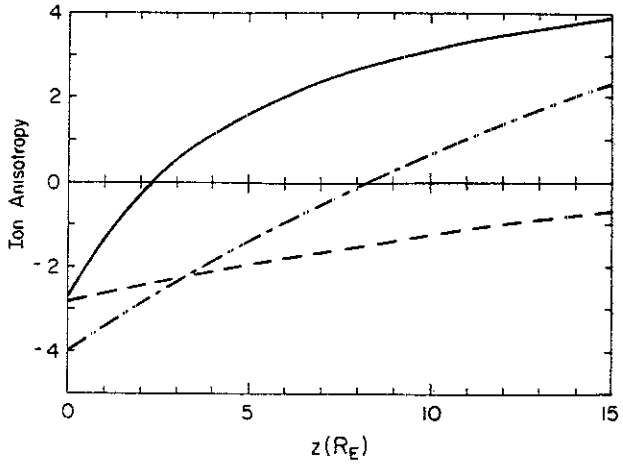

Fig. 4. The predicted anisotropies of 30-keV protons (solid curve), 60-keV protons (dashed curve) and 30 keV/Q helium (dash-dot curve) versus distance from the bow shock in units of R_E.

shown in Figure 1. It is evident in Figure 5 that the ion-excited differential wave intensity decreases rapidly with increasing z as observed; somewhat beyond ISEE 3 ($\simeq 200\ R_E$), (28) actually predicts less intensity than in interplanetary space. The wave deficit, which arises from the condition $I_+^0(k) \simeq 0$, results in the free-streaming ion distributions for $E < E_c$. The spectra are dominated by helium (protons) for $\nu < (>) \sim 1.1 \times 10^{-2}$ Hz corresponding to ~44-keV protons and ~22-keV/Q helium.

Equation (28) may be expanded for small z as

$$I_\pm(k, z) = |\alpha_p(k) f_p(|\Omega_p/k|, 0) + \alpha_{He}(k) f_{He}(|\Omega_{He}/k|, 0) - I_-^0(k)|[1 \pm z l^{-1}(k)]^{-1}$$

$$l^{-1}(k) \equiv \tfrac{1}{2} V[(K_{\parallel,p}{}^0)^{-1}(1 + \psi_p)]_{v=|\Omega_p/k|} [\alpha_p(k) f_p(|\Omega_p/k|, 0) + \alpha_{He}(k) f_{He}(|\Omega_{He}/k|, 0)] \quad (36)$$

where $l(k)$ is the scale length for decrease or increase in the wave intensity away from the bow shock. Where the ion excited waves dominate the interplanetary spectrum ($\Sigma_s \alpha_s f_s \gg I_-^0$), $l(k) \simeq L(v = |\Omega_p/k|)$, indicating that the wave intensity and the proton omnidirectional distribution at the corresponding energy decrease together. We note further that $\gamma_\pm(k, z = 0) = \pm \frac{1}{2} V l^{-1}(k)$, so that wave growth rates at the bow shock can be calculated immediately. At $\nu \simeq 1.3 \times 10^{-2}$ Hz, corresponding to 30-keV protons, $\gamma_+ \simeq 5.6 \times 10^{-3}$ s^{-1}. The real part of the wave frequency in the solar wind frame $\omega = kV_A \simeq 8.2 \times 10^{-3}$ s^{-1}, comfortably larger than γ as formally required for the validity of quasilinear theory. For $\nu < 1.3 \times 10^{-2}$ Hz, γ decreases rapidly; for $\nu > 1.3 \times 10^{-2}$ Hz, however, γ increases rapidly, surpassing ω and severely pressing the limits of quasilinear theory.

In Figure 6 we compare the wave spectra predicted at $z = 0$ and $z = 2R_E$ with a power spectrum typical of disturbed upstream conditions taken from OGO 5 [*Childers and Russell*, 1972] (dash-dot-dot line). The observed spectrum included power in the radial component of the magnetic field only; assuming approximate isotropy we have multiplied by a factor of 3 to obtain the total power. The predicted spectra are presented for both values of z because they are clearly sensitive to z near $\nu \simeq 3 \times 10^{-2}$ Hz, yet the exact location of the bow shock during the time interval utilized to obtain the measured power spectrum is uncertain.

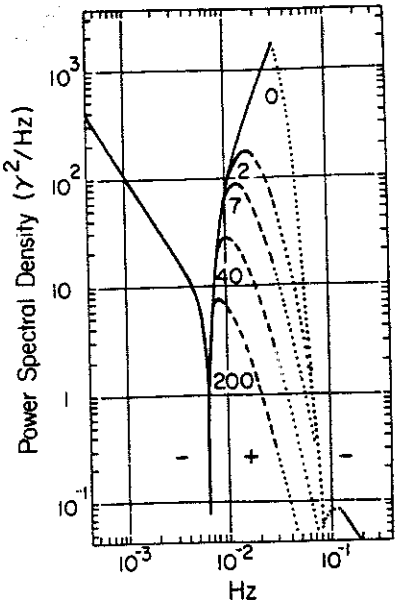

Fig. 5 The predicted power spectral density at several distances from the bow shock in units of R_E. The dashed portion of each curve indicates that range of frequency for which the ion distribution at the corresponding energy does not decrease rapidly with energy as assumed. The dotted portions of each curve indicate schematically the precipitous decrease in power for $\nu > 0.03$ Hz followed by an increase to the interplanetary power spectral density. The plus sign denotes ion-excited waves propagating upstream relative to the solar wind. The negative sign denotes partially damped interplanetary waves propagating toward the bow shock.

The agreement is qualitatively good. In overall power level, minimum power at ~6–7 × 10^{-3} Hz, and maximum power at ~2–3 × 10^{-2} Hz, the observed and predicted spectra are in good agreement. Power minima and maxima at these frequencies appear to be ubiquitous features of more recently analyzed upstream wave spectra (M. M. Hoppe, private communication, 1981). However, the OGO 5 spectrum is much broader than those predicted. The observed excess power at higher frequencies is certainly due in part to the formation of shocklets [*Hoppe et al.*, 1981], a nonlinear cresting of the large-amplitude compressive hydromagnetic waves that transfers power to higher frequencies and that is not included in the theory. Similarly, the excess power at lower frequencies could be due to a nonlinear wave-particle or wave-wave interaction resulting in a cascade of power to lower frequencies.

The predicted wave polarization is also consistent with observations. The even dependence of $I(k, z)$ on k implies linear polarization on average, or zero helicity. From observations of shocklets linear polarizations are generally inferred, although net helicity also occurs [*Hoppe et al.*, 1981]. It is clear from equation (A6) that a net helicity results if the ion distribution, $F_s(v, \mu)$, is not linear in μ as assumed in section 5. Indeed, a different approach to determining the μ dependence of $F_s(v, \mu)$, subject to the constraints that the omnidirectional distribution and streaming are specified, has been suggested by *Stevens and van Rooijen* [1981*b*] in a different context. They demonstrate that maximizing entropy leads to a 'most likely' distribution of the form $F_s(v, \mu) = A \exp(B\mu)$, where $A(v)$ and $B(v)$ are determined by the two constraints. Such a distribution would favor right-hand circularly polarized waves in the solar wind frame.

It is of interest to compute the predicted energy densities in diffuse upstream protons ($\equiv U_p$) and in upstream hydromagnetic waves ($\equiv U_{\delta B}$) at the bow shock. With U_p defined by $U_p \equiv \int_{v_p^0}^{\infty} dv (4\pi v^2)(\frac{1}{2} m_p v^2) f_p(v, 0)$, a numerical integration utilizing our assumed parameters yields $U_p = 3.5 \times 10^2$ eV cm^{-3}. The energy density in diffuse protons with energies greater than 15 keV is predicted to be 2.1×10^2 eV cm^{-3}, in excellent agreement with the typical observed value of 200 eV cm^{-3} [*Ipavich et al.*, 1981*b*]. Since $f_s(v, z)$ is predicted to be continuous across the bow shock the same energy density in 'diffuse' ions should be present in the magnetosheath. For the purpose of calculating the energy density in hydromagnetic waves we may neglect the interplanetary spectrum, $I_-^0(k)$, in comparison with $\Sigma_s \alpha_s(k) f_s(|\Omega_s/k|, 0)$ (see equation (25)). Then with $U_{\delta B} \simeq (4\pi)^{-1} \Sigma_s \int_0^{k_s^0} dk \alpha_s(k) f_s(|\Omega_s/k|, 0)$, where $k_s^0 = |\Omega_s/v_s^0|$, we obtain the analytical expression

$$U_{\delta B}/U_p \simeq \frac{3.6}{6.5.7} \beta^2 V_A V^{-1} u_p^4 / \langle v^4 \rangle \qquad (37)$$

where we have taken for simplicity $(v_{\mathrm{He}}^0)^2 = \frac{1}{2}(v_p^0)^2$ and where $\langle v^4 \rangle \equiv \int_{v_p^0}^{\infty} dv v^4 f_p(v, 0) [\int_{v_p^0}^{\infty} dv\, f_p(v, 0)]^{-1}$. We have evaluated $\langle v^4 \rangle$ numerically: $\langle v^4 \rangle = 0.274\, u_p^4$. Substituting the assumed values of the parameters we obtain $U_{\delta B}/U_p \simeq 7.2 \times 10^{-2}$ and $U_{\delta B} \simeq 25$ eV cm^{-3}. Analysis of the observed magnetic field fluctuations typically shows that $|\delta \mathbf{B}|_{\max} \simeq B$ so that $U_{\delta B} \simeq \frac{1}{2} B^2 (8\pi)^{-1} \simeq 30$ eV cm^{-3}, in respectable agreement with the theoretical prediction.

We now present a few miscellaneous results of the theory. From (14), the value of the proton distribution function evaluated at 30 keV as inferred from observations, and the assumed value of v_p^0 corresponding to a 5-keV proton, the rate at which 5-keV protons must be 'injected' at the shock front per unit area [$= 4\pi (v_p^0)^2 N_p$ protons cm^{-2} s^{-1}] may be evaluated and yields $\simeq 5.2 \times 10^5$ protons cm^{-2} s^{-1}. With a

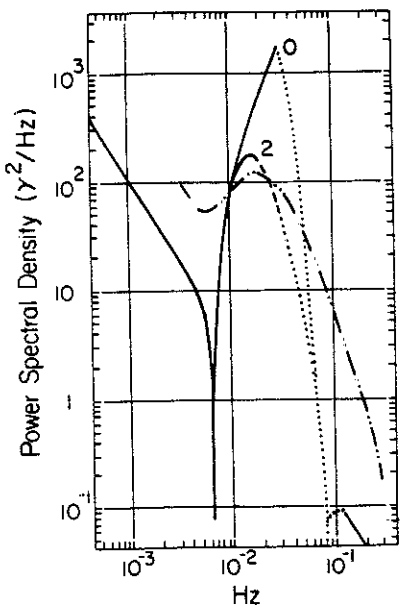

Fig. 6. The predicted power spectral density at the bow shock and 2 R_E upstream compared with a power spectral density (dash-dot-dot curve) typical of disturbed upstream conditions taken from OGO 5 measurements [*Childers and Russell*, 1972]. The dashed and dotted portions of the predicted curves are as described in Figure 5. The observed density (in the radial component of the magnetic field) has been multiplied by a factor of 3 to obtain total power under the assumption of isotropy.

proton density in the solar wind of $\simeq 8$ protons cm^{-3} implying a solar wind proton flux of $\simeq 3.2 \times 10^8$ protons cm^{-2} s^{-1}, the theoretically predicted 'injection' flux requires that approximately 1 proton in 600 must either be reflected from the solar wind or leak back upstream from the magnetosheath.

It is instructive to evaluate the derived proton diffusion coefficients at the shock; their dependence on z follows directly from that of the differential wave intensities. The parallel diffusion coefficient, $K_{\parallel,p}(v, 0) = K_{\parallel,p}{}^0(v)[\alpha_p(\Omega_p/v)f_p(v, 0) + \alpha_{He}(\Omega_p/v)f_{He}(v\Omega_{He}/\Omega_p, 0) - I_-{}^0(\Omega_p/v)]^{-1} = \frac{1}{2}VL(v)(1 + \psi_p)$, which increases approximately exponentially with energy for $E < E_c$. At 30 keV, $K_{\parallel p}(z = 0) \simeq 1.9 \times 10^{17}$ cm^2 s^{-1}. From (4) and (6)

$$\left(\frac{K_{\perp,p}}{K_{\parallel,p}}\right)_{z=0} = \left(\frac{1}{\xi_1(1 + \psi_p)}\right)^2 \left(\frac{a}{L(v)}\right)^2 \left(\frac{E}{E_0}\right)^2 \qquad (38)$$

which equals $\simeq 0.14$ at 30 keV and decreases rapidly with increasing energy for $E < E_c$. The ratio also decreases rapidly with increasing z. From $K_{\parallel,p}$ we can determine the scattering mean free path, λ, via $K_{\parallel} = \frac{1}{3}\lambda v$. At the shock front, $\lambda/L(v) = \frac{3}{2}(1 + \psi_p)(V/v)$, which equals $\simeq 0.66$ for 30-keV protons, but increases to $\simeq 1$ for either 7.5-keV protons or 280-keV protons. Again, we are clearly pressing the limits of diffusion theory, which formally requires $\lambda \ll L$. It should also be noted that the derived v dependence of $K_{\parallel,p}$ differs greatly from those ad hoc dependences assumed by *Lee et al.* [1981], *Terasawa* [1981], *Forman* [1981], and *Ellison* [1981].

7. Limitations and Conclusions

We have presented a theoretical model for the self-consistent behavior of hydromagnetic waves and 'diffuse' ions upstream of the earth's bow shock in the quasi-equilibrium that results when the interplanetary magnetic field and the solar wind velocity are approximately parallel. Apart from parameters that describe the solar wind and bow shock such as $|\mathbf{V}|$, $|\mathbf{B}|$, shock compression and the lateral distance to field lines that are not connected to the bow shock, the only 'free' parameters governing the waves and ions that must be taken from observations are the differential intensities of the ion species at one reference energy at the bow shock (here we have chosen 30 keV/Q).

In spite of the paucity of free parameters, as described in detail in section 6, the theory is remarkably successful in explaining quantitatively many of the observed features of the hydromagnetic waves and diffuse ions: notably

1. The ion energy spectra near the bow shock are exponential in energy per charge for $E/Q \gtrsim 30$ keV/Q with the same e folding E/Q for all species ($\sim$20 keV/Q).

2. Near the bow shock the ion intensities decrease with distance from the shock front with a scale length of 5–7 R_E for 30-keV protons

3. The ion intensities are further reduced, and the spectra harder, at the orbit of ISEE 3 ($\sim$ 200 R_E)

4. The proton anisotropy at 30 keV is ~ -0.28 at the bow shock, indicating streaming into the magnetosphere passes through zero at $\sim$ 2.4 R_E and increases at larger distances to the asymptotic limit 0.51, indicating large streaming away from the bow shock.

5. The wave intensity spectra near the bow shock are modified from the interplanetary spectrum in the range $5 \times 10^{-3} - 10^{-1}$ Hz with minimum power at $\sim 6 \times 10^{-3}$ Hz, maximum power at $\sim$ 2–3 $\times 10^{-2}$ Hz, and a precipitous decay in power beyond 3×10^{-2} Hz.

6. The wave intensity spectrum in the frequency range 6×10^{-3}–10^{-1} Hz decreases with distance from the shock front together with the ion densities and actually falls below interplanetary levels beyond ISEE 3.

7. The waves are linearly polarized on average.

8. The total energy density in protons with $E > 15$ keV at the bow shock is typically 200 eV cm^{-3}.

9. The total energy density in waves with frequencies in the range 6×10^{-3}–4×10^{-2} Hz at the bow shock is typically 25 eV cm^{-3}.

The theory also predicts:

1. The rate at which ions must be 'injected' (presumably via reflection out of the solar wind or leakage from the downstream magnetosheath) at the shock front: $\sim 5 \times 10^5$ protons cm^{-2} s^{-1}.

2. The spatial and energy dependence of the spatial diffusion coefficients parallel and perpendicular to the interplanetary magnetic field.

The quantitative agreement between theory and observations is particularly remarkable since a number of approximations and simplifications, some of which are in part not formally justified, have been made to yield analytical expressions for the ion distributions and wave intensities:

1. Ion transport is based on diffusion equations that require (1) that the scattering mean free path be much less than the spatial scale-length and (2) that the ion speed be much greater than the solar wind speed. Requirement (1) is severely pressed as discussed quantitatively in section 6. Requirement (2) is weakly satisfied at the observed 'injection' energies.

2. The assumed forms of the spatial diffusion coefficients are based on quasilinear theory, which requires (1) that the magnitude of the magnetic field fluctuations be small in comparison with that of the mean field and (2) that the wave growth rates be substantially less than the wave frequencies in the solar wind frame. Requirement (1) is not satisfied by the upstream hydromagnetic waves as indeed predicted by the theory. Requirement (2) is not satisfied at the higher frequencies ($\nu \gtrsim$ 1–2 $\times 10^{-2}$ Hz).

3. The assumption that the spatial diffusion coefficients are independent of the spatial coordinates normal to the magnetic field is suspect but necessary to perform the eigenfunction expansion in the radial coordinate r. The $J_0(\xi_1 r a^{-1})$ dependence on r must, therefore, be viewed as approximate

4. The replacement of the pitch angle diffusion coefficient, $D_\mu(\mu)$, in (3) by $D_\mu(\pm 1)$ for $\mu \gtrsim 0$ is motivated by the observed shoulder in the wave intensity in the frequency range 4×10^{-3}–4×10^{-2} Hz but is not well justified by the derived wave intensity that depends sensitively on frequency.

5. The evaluation of the wave growth rate $\gamma(k)$ in (15) in terms of the ion distributions at the lowest energy that can resonate with waves at that frequency (equation (22)) is an approximation that depends on $K_{\parallel,s}\partial f_s/\partial z$ being a rapidly decreasing function of v. It is clear from Figure 1 that this approximation is only formally valid above an energy ($\sim$ 30-keV protons at ~ 7 R_E) which depends on distance from the bow shock and ion species.

Approximations (4) and (5) together result in a one-to-one correspondence between wave frequency and ion energy

given by the cyclotron resonance condition for low frequency waves at pitch angles of 0° or 180° ($kv = \pm \Omega_s$). This correspondence, which is an essential feature of *Skilling* [1975], simplifies the problem to one amenable to analytical techniques. Clearly the approximation is valid only if the spectra are sufficiently smooth. The singular behavior of the proton distribution at $E = E_c$ apparent in Figure 1 results directly from the zero in the wave intensity at the corresponding frequency and is therefore an artificiality resulting from the approximation.

6. The assumption that the ion phase-space distribution function $F_s(v, \mu)$, is linear in μ yields a growth rate even in k (see equation (15)), which guarantees equal differential intensities of right-hand and left-hand circularly polarized waves in general agreement with observations [*Hoppe et al.*, 1981]. A small quadratic dependence of $F_s(v, \mu)$ on μ would favor one polarization or the other depending on the sign of the quadratic dependence, thus providing an explanation for the fact that occasionally a net helicity is observed [*Hoppe et al.*, 1981].

7. The simplifying assumption that all wave vectors are parallel to **B** precludes an explanation of the observed compression of the upstream waves. However, the general success of the theory in explaining the basic features of the coupled wave-ion system indicates that the compressive nature of the waves is not essential to the basic wave-ion interaction apart from contributing to the effective mirror reflection of ions through 90° pitch angle, an effect we have included heuristically in deriving the spatial diffusion coefficients. This statement is supported by the noncompressive nature of the waves observed in association with the 'intermediate' ion distributions indicative of an earlier stage in the evolution when wave vectors are more nearly parallel to **B** and presumably before nonlinear effects have broadened the wavevector distribution and increased the compression.

8. Damping of the upstream hydromagnetic waves on the solar wind plasma is neglected although it may play a role [*Auer et al.*, 1976].

9. Diffusive transport of the ions in the magnetosheath is neglected.

10. Nonlinear wave-particle and wave-wave effects that can transfer power in frequency are neglected in the theory. Such effects are presumably in part responsible for the lack of overall quantitative agreement evident in Figure 6 between the derived spectra and the representative observed spectrum. There is clear evidence for the formation of shocklets, which transfers power to higher frequencies and is presumably responsible for the discrepancy at frequencies $\nu \gtrsim 3 \times 10^{-2}$ Hz. The nonlinear wave-particle interaction is expected to transfer power to lower frequencies [*Lee and Völk*, 1973] and may be responsible for the discrepancy at frequencies $\nu \lesssim 8 \times 10^{-3}$ Hz. It is also possible, however, that relieving the one-to-one correspondence between frequency and energy by numerically improving on approximations (4) and (5) will partially eliminate the discrepancies without resort to nonlinear phenomena. We also look forward to future observations and analysis of upstream wave spectra in order to make more extensive and detailed statistical comparisons as has been possible for the ion distributions.

11. The theory assumes the 'injection' of seed ions of speed v_s^0 at the shock front at a rate $4\pi(v_s^0)^2 N_s$ cm^{-2} s^{-1}. The most likely source of the seed ions is either (1) via direct reflection out of the solar wind at the shock front such that the reflection is elastic in the frame moving along the shock front in which $\mathbf{V} \times \mathbf{B} = 0$ [*Sonnerup*, 1969; *Paschmann et al.*, 1980], or (2) via leakage back upstream from the shock-heated magnetosheath [*Edmiston et al.*, 1982]. Although in principle N_s is determined by the structure of the bow shock, the transport of these low energy ions (1–6 keV/nucleon) cannot be treated within a diffusion theory as we have presented. Accordingly we have modelled the initial acceleration and transport out of the solar wind or magnetosheath as monoenergetic injection at the shock front for the subsequent shock acceleration and wave excitation addressed by this theory.

From equations (14), (27), (28), and (31) it is clear that the ion and wave spectra are independent of v_s^0 except for overall normalization that, however, is taken from observations. Accordingly, the spectra in Figures 1, 2, and 5 can simply be extended to lower energy per charge and higher frequency in order to consider smaller injection speeds v_s^0. The extensions for $z \neq 0$, however, suffer the same quantitative limitation as the dashed portions of the spectra since, at small v, $K_{\parallel,s}\partial fs/\partial z$ is not a rapidly decreasing function of energy as assumed in deriving the wave growth rates. The inferred injection rate $4\pi(v_s^0)^2 N_s$, of course, does depend on v_s^0. The insensitivity of the ion and wave spectra to v_s^0 also supports the simplifying assumption that the injection is monoenergetic.

12. As discussed in section 3 this theory treats the quasi-equilibrium that results when the angle θ between **B** and **V** is small so that the connection time of the magnetic field line passing through the point of observation to the nose of the bow shock is sufficiently long. The existence of a quasi-equilibrium is supported by the observed 'plateaus' in ion intensity, which also indicate that the configuration is insensitive to small changes in magnetic field direction and shock structure over that portion of the bow shock accessible via magnetic connection to the observing spacecraft. To the extent that these changes do have a small effect on the upstream ion and wave spectra we have used the term quasi-equilibrium. By taking $\theta = 0$ (infinite connection time) we have not only suppressed these temporal variations but also necessarily neglected both the effects of field line convection across the shock front and the approach to the quasi-equilibrium.

The time scale for the approach to the quasi-equilibrium however, can be estimated from observations and the theory. The requirement that $\theta \lesssim 50°$ in order to observe ions at ~ 30 keV/Q implies a characteristic acceleration time to 30 keV/Q of roughly 5 min. Characteristic theoretical time scales are γ^{-1} to excite the hydromagnetic waves, $L^2 K_{\parallel}^{-1}$ to develop the predicted spatial dependence parallel to the magnetic field $L(\Delta V)^{-1}$ to gain the specified energy and $a^2 K_{\perp}^{-1}$ to develop the predicted spatial dependence normal to the magnetic field. Here L is the characteristic ion scale length parallel to **B** as defined in (33) and $\Delta V \equiv \hat{n} \cdot (\mathbf{V}_u - \mathbf{V}_d)$, where $\mathbf{V}_u$ and $\mathbf{V}_d$ are the upstream and downstream flow velocities and $\hat{n}$ is the shock normal unit vector. For 30-keV protons and the corresponding wave frequency (1.3×10^{-2} Hz) the four time scales are respectively 3 min, 1 min, 2 min, and 26 min, in reasonable agreement with the observed time scale: wave growth followed by ion acceleration requires roughly 3 min + 2 min = 5 min. The larger magnitude of the fourth time scale implies that the spatial evolution of the

spectra normal to the magnetic field toward the quasi-equilibrium configuration takes substantially longer than that parallel to the field, but presumably, the quasi-equilibrium configuration parallel to the field is insensitive to this delay. However, it should be noted, as discussed previously, that the spatial structure normal to the field cannot be interpreted quantitatively within this model since the r dependence of the wave intensity has been neglected.

Without calculating the evolution of the wave and ion spectra toward the quasi-equilibrium it is difficult to assess whether the spectra for finite connection times bear significant resemblance to those of the quasi-equilibrium configuration. For example, observations that the relative ion abundances are fixed as functions of E_s/Q_s during the approach to the quasi-equilibrium [*Ipavich et al.*, 1981*b*] indicate that this feature of the quasi-equilibrium holds for smaller connection times. Clearly an investigation of the connection time dependent evolution of the wave and ion spectra is required to address these issues. *Skadron and Lee* [1982] are currently investigating the evolution of the ion spectra with increasing connection time for a linear system in which the spatial diffusion coefficients are specified.

13. The theory assumes that the solar wind is infinitely massive: **V** is specified with no consideration of the influence of the upstream ions and waves on the solar wind flow. Since the pressure of the upstream protons dominates that of the upstream waves and minor ions, the modification of the solar wind flow in the foreshock, neglecting V_x and V_y, may be estimated by

$$\rho_0 V dV/dz \simeq -\tfrac{2}{3}\, dU_p/dz \tag{39}$$

where ρ_0 is the solar wind mass density. Since $\rho_0 V$ is then approximately constant, (39) yields

$$V_\infty - V(z) \simeq \tfrac{2}{3}\, U_p(z)(\rho_{0,\infty} V_\infty)^{-1} \tag{40}$$

where $\rho_{0,\infty}$ and V_∞ are limiting values as $z \to \infty$. With $U_p(0) \simeq 350$ eV cm^{-3}, $\rho_{0,\infty} \simeq 10\, m_p$ cm^{-3} and $V_\infty \simeq 4 \times 10^7$ cm s^{-1}, we have $V_\infty - V(0) \simeq 6$ km s^{-1} at the bow shock, in qualitative agreement with values inferred observationally [*Bame et al.*, 1980].

In view of these simplifications, approximations, and assumptions, the theory should be viewed as a model that incorporates and elucidates the major features of the wave-ion interaction within the quasi-equilibrium configuration. But it is a model that is remarkably successful in reproducing the extensive observations afforded in particular by the ISEE missions and that indicates directions for more refined studies of the quasi-equilibrium and pioneering studies of the approach to the quasi-equilibrium. Studies of the time development on a given field line, as it convects along the shock front, of the hydromagnetic waves and energetic ions provide a unique opportunity within astrophysics to test time-dependent quasilinear theory, investigate the development of hydromagnetic turbulence, and understand the acceleration of energetic particles by astrophysical shocks. It should be possible to follow and understand the initial generation of the reflected component, the initial growth of right-hand circularly polarized (in the solar wind frame) waves, the disruption of the reflected ion beam by the waves to form the intermediate particle distribution, the generation of left-hand circularly polarized waves as ions are scattered back toward the bow shock, the further growth of the waves to sufficiently large amplitude that nonlinear processes become important, the disappearance of the reflected ions by further scattering, and the appearance of the accelerated diffuse ions. Satellite measurements provide a comprehensive album of 'snapshots' portraying the development at all stages. Interestingly, it is the finite size of the bow shock that limits its prowess as a particle accelerator to soft exponential ion spectra, but which affords an opportunity to study the time-dependent development of the wave-ion processes and more severely test our theoretical understanding.

Finally, a noteworthy feature of the theory is the importance of helium in determining the wave spectrum at frequencies less than $\sim 1.1 \times 10^{-2}$ Hz in spite of its differential intensity being about 7% that of protons at a given E_s/Q_s. The dominance of helium at low frequencies arises from the cyclotron resonance condition $kv \simeq \Omega_s$, which dictates that helium resonant with a given wave number has half the energy per charge of protons resonant with the same wave number. The approximately exponential spectra in energy per charge then result in the dominance of helium at low frequencies corresponding to high energies. The role of helium in the excitation of upstream hydromagnetic waves has been overlooked in previous work: *Barnes* [1970], *Gary et al.* [1981], and *Sentman et al.* [1981*a*, *b*]. There is, of course, very little total magnetic field power in the frequency interval dominated by helium (6×10^{-3}–1.1×10^{-2} Hz). A nonlinear cascade of power from the proton-dominated peak (1.1×10^{-2}–4×10^{-2} Hz) to lower frequency could overpower the helium-excited waves. A possible diagnostic of the importance of such a cascade presents itself: The power spectrum in the frequency range 6×10^{-3}–1.1×10^{-2} Hz should be sensitive to the helium abundance (which typically varies between 1% and 15%) if the nonlinear transfer of power into that range is unimportant, but insensitive if the transfer is important.

APPENDIX

The quasilinear evolution of the cylindrically symmetric, spatially homogeneous phase-space distribution function $F_s(p_\parallel, p_\perp, t)$ of particle species s in the presence of (possibly unstable) electromagnetic waves propagating parallel and antiparallel to an ambient magnetic field $B\hat{e}_z$ is given by *Lee* [1971] (his equation (49), term (49.5)) as

$$\frac{\partial F_s}{\partial t} = \frac{q_s^2}{2p_\perp} Re\, i \int_{\mathfrak{D}} dk \sum_{\rho=\pm} \frac{(\omega_\rho)^2}{c^2 k^2} G^\rho \left[\frac{p_\perp I^\rho(k)(G^\rho F_s)}{\omega^\rho - k v_z + \Omega_s} \right] \tag{A1}$$

where $p_\parallel$ and $p_\perp$ are the components of the particle momentum parallel and perpendicular to the ambient field, v is particle speed, $\Omega_s (\equiv q_s B/\Gamma m_s c)$ is the particle gyrofrequency, q_s and m_s are, respectively, the charge and mass of species s, $\Gamma \equiv (1 - v^2 c^{-2})^{-1/2}$, and the operator $G^\rho \equiv \partial/\partial p_\perp + (k/\omega^\rho)(v_\perp \partial/\partial p_z - v_z \partial/\partial p_\perp)$. The wave power spectrum $I^\rho(k)$ [$\propto \langle |\delta\tilde{B}_x - i\delta\tilde{B}_y|^2 \rangle$, where $\delta\tilde{\mathbf{B}}(k, \omega^\rho)$ is the transformed fluctuating magnetic field and the angle brackets denote ensemble average, brackets denote the differential intensity of the least stable wave with $Re\,\omega \gtrless 0$ ($\rho = \pm$, $\omega = \omega^\mp$) normalized such that the ensemble-averaged square of the fluctuating magnetic field, $\langle \delta\mathbf{B} \cdot \delta\mathbf{B} \rangle$ equals $\Sigma_{\rho=\pm} \int_{-\infty}^{\infty} dk\, I^\rho(k)$. The symbol $\mathfrak{D}$ indicates that the integration path of $kv_z/|v_z|$ runs below the zeroes of the denominator, $(\omega^\rho - kv_z + \Omega_s)$. In what follows we restrict ourselves to the nonrelativis-

tic limit and hydromagnetic waves. From the definition of $I^\rho(k)$ in terms of $\langle|\delta\bar{B}_x - i\delta\bar{B}_y|^2\rangle$ and the convention that fluctuating quantities vary as $\exp(-i\omega t)$, we note that $I^+(k)$ is right-hand circularly polarized and $I^-(k)$ is left-hand circularly polarized, with respect to the ambient field for $B > 0$. The polarizations are reversed for $B < 0$.

The wave frequencies, ω^ρ, are given by the least stable roots of (see *Lee* [1971], equation (28))

$$D \equiv \omega^2 - c^2k^2 + 4\pi^2\omega \sum_s q_s^2 \int dv_z dv_\perp\, v_\perp^2\, (GF_s)(\omega - kv_z + \Omega_s)^{-1} \quad \text{(A2)}$$

where F_s is normalized so that $\int d^3\mathbf{v}\, F_s = n_s$, the number density of particle species s. By causality $D(\omega)$ is defined for $Im\omega > 0$ and must be analytically continued into the lower-half ω-plane. Thus, for real ω, $(v_z - \omega/k - \Omega_s/k)^{-1} = P(v_z - \omega/k - \Omega_s/k)^{-1} + i\pi k|k|^{-1}\delta(v_z - \omega/k - \Omega_s/k)$, where the symbol P denotes principal value:

$$D = \omega^2 - c^2k^2 + 4\pi^2\omega \sum_s q_s^2 \int dv_z\, dv_\perp\, v_\perp^2\, (GF_s)P(\omega - kv_z + \Omega_s)^{-1} - 4\pi^3(\omega/k)ik|k|^{-1} \sum_s q_s^2 \int dv_z\, dv_\perp\, v_\perp^2\, (GF_s)\delta(v_z - \omega/k - \Omega_s/k) \quad \text{(A3)}$$

In application to the upstream hydromagnetic waves in the solar wind the principal value term in expression (A3) is dominated by the nearly isotropic solar wind plasma for which $G \simeq \partial/\partial p_\perp$ and $P(\omega - kv_z + \Omega_s)^{-1}$ is expandable in powers of $kv_z(\omega + \Omega_s)^{-1}$. The final term in expression (A3) is dominated by the upstream energetic ions for which $v \gg \omega/k$ and $G \simeq (k/\omega)(v_\perp\partial/\partial p_z - v_z\partial/\partial p_\perp)$. Assuming $|\omega| \ll |\Omega_s|$, expression (A3) then simplifies to

$$D \simeq \omega^2\,(1 + c^2/V_A^2) - k^2c^2 - 4\pi^3\, i\, k|k|^{-1} \sum_s q_s^2 m_s^{-1} \int dv d\mu v^2\, (1 - \mu^2)(\partial F_s/\partial\mu)\delta(\mu - \Omega_s/kv) \quad \text{(A4)}$$

where $V_A(V_A^2 = B^2/4\pi\,\Sigma_s\, m_s n_s)$ is the Alfvén speed, $\mu = v_z v^{-1}$, and $F_s(\mu, v)$ is the distribution function of energetic ion species s. The roots $\omega^\rho(=\omega_0 + i\gamma)$ of $D(\omega) = 0$ are found by equating real and imaginary parts in expression (A4):

$$\omega_0^2 = k^2V_A^2 + \gamma^2 \quad \text{(A5)}$$

$$\gamma = \frac{2\pi^3}{|k|}\frac{k}{\omega}\frac{V_A^2}{c^2}\sum_s \frac{q_s^2}{m_s}\int dv d\mu v^2(1 - \mu^2)\frac{\partial F_s}{\partial\mu}\,\delta(\mu - \Omega_s/kv) \quad \text{(A6)}$$

Assuming that $\partial F_s/\partial\mu$ does not change sign, its sign determines the direction of the energetic ion streaming. Assuming all ions stream in the same direction, waves that propagate in the direction of the ion streaming are unstable and waves which propagate in the opposite direction are stable. Technically, there is a streaming threshold for instability equal to the Alfvén speed that arises by including the term $\partial/\partial p_\perp$ in G when calculating ImD. The threshold is negligible in application to upstream ions.

Returning now to (A1), the evolution of the upstream energetic ions is dominated by the resonant denominator, which may be replaced by a delta function if $|\gamma| \ll |\Omega_s|$. Again approximating $G^\rho \simeq (k/\omega^\rho)(v_\perp\partial/\partial p_z - v_z\partial/\partial p_\perp)$ and noting the deformation $\mathfrak{D}$ of the k contour, equation (A1) may be rewritten as

$$\frac{\partial F_s}{\partial t} = \frac{\pi}{2}\frac{\Omega_s^2}{B^2}\frac{\partial}{\partial\mu}\sum_{\rho=\pm}\int_{-\infty}^{\infty} dk(1 - \mu^2)I^\rho(k)\frac{\partial F_s}{\partial\mu}\,\delta(\omega^\rho - kv_z + \Omega_s) \quad \text{(A7)}$$

which describes diffusion in μ space with diffusion coefficient

$$D_\mu = \frac{\pi}{2}\frac{\Omega_s^2}{B^2}\frac{(1 - \mu^2)}{v|\mu|}\sum_{\rho=\pm} I^\rho\left(\frac{\omega^\rho + \Omega_s}{v_z}\right) \quad \text{(A8)}$$

For application to upstream waves and ions the natural distinction in wave intensities is according to the direction of the wave phase speed, ω_0/k, which together with the sign of $\partial F_s/\partial\mu$ determines instability or stability, rather than according to polarization. We therefore define the differential intensities $I_\pm(k)$ for $(\omega_0/k) \gtrless 0$, in terms of which

$$D_\mu = \frac{\pi}{2}\frac{\Omega_s^2}{B^2}\frac{(1 - \mu^2)}{v|\mu|}\sum_{+,-} I_\pm\left(\frac{\Omega_s}{v\mu}\right) \quad \text{(A9)}$$

where we have neglected ω^ρ compared with Ω_s. $I_+(k)$ is the intensity of waves propagating in the $\hat{e}_z$ direction with $k > 0 (k < 0)$ corresponding to right-hand (left hand) circularly polarized waves for $B > 0$ and the reverse polarizations for $B < 0$. $I_-(k)$ is the intensity of waves propagating in the $-\hat{e}_z$ direction with $k > 0$ ($k < 0$) corresponding to left-hand (right hand) circularly polarized waves for $B > 0$ and the reverse polarizations for $B < 0$.

Acknowledgments. The author wishes to express special thanks to L. A. Fisk, M. L. Goldstein, J. V. Hollweg, M. M. Hoppe, F. M. Ipavich, I. Lerche, M. Scholer, and G. Skadron for their continued support through numerous informative discussions. He is particularly thankful to F. M. Ipavich for emphasizing the potential importance of helium. He is also grateful to P. A. Isenberg for critically reading the original typescript and J. Perko for numerically evaluating the analytical expressions. This work was supported in part by the NASA Solar-Terrestrial Theory Program grant NAGW-76, by NASA grants NSG-7411 and NAS-5-20062, and by NSF grant ATM 8109545.

The editor thanks D. Eichler, D. D. Sentman, and F. M. Ipavich for their assistance in evaluating this paper.

REFERENCES

Anderson, K. A., A review of upstream and bow shock energetic particle measurements, *Nuovo Cimento, 2C*, 747, 1979.

Argo, H. V., J. R. Asbridge, S. J. Bame, A. J. Hundhausen, and I. B. Strong, Observations of solar wind plasma changes across the bow shock, *J. Geophys. Res., 72*, 1989, 1967.

Asbridge, J. R., S. J. Bame, and I. B. Strong, Outward flow of protons from the earth's bow shock, *J. Geophys. Res. 73*, 577, 1968.

Asbridge, J. R., S. J. Bame, J. T. Gosling, G. Paschmann, and N. Sckopke, Energetic plasma ions within the earth's magnetic sheath, *Geophys. Res. Lett.*, *5*, 953, 1978.

Auer, R.-D., H. Grünwaldt, and H. Rosenbauer, Bow-shock-associated proton heating in the upstream solar wind, *J. Geophys. Res., 81*, 2030, 1976.

Axford, W. I., E. Leer and G. Skadron, The acceleration of cosmic rays by shock waves, *Proc. Int. Conf. Cosmic Rays 15th, 11*, 132, 1977.

Bame, S. J., J. R. Asbridge, W. C. Feldman, J. T. Gosling, G. Paschmann, and N. Sckopke, Deceleration of the solar wind upstream from the earth's bow shock and the origin of diffuse upstream ions, *J. Geophys. Res., 85*, 2981, 1980.

Barnes, A., Theory of generation of bow-shock-associated hydromagnetic waves in the upstream interplanetary medium, *Cosmic Electrodyn., 1*, 90, 1970.

Belcher, J. W., and L. Davis, Jr., Large-amplitude Alfvén waves in the interplanetary medium, 2, *J. Geophys. Res., 76*, 3534, 1971.

Bell, A. R., The acceleration of cosmic rays in shock fronts, I, *Mon. Not. R. Astron. Soc., 182*, 1978.

Bonifazi, C., and G. Moreno, Reflected and diffuse ions backstreaming from the earth's bow shock, 1, Basic properties, *J. Geophys. Res., 86*, 4397, 1981.

Childers, D. D., and C. T. Russell, Power spectra of the interplanetary magnetic field near the earth, in *Solar Wind, NASA Spec. Publ. 308*, p. 375, 1972.

Earl, J. A., The diffusive idealization of charged-particle transport in random magnetic fields, *Astrophys. J., 193*, 231, 1974.

Eastman, T. E., R. R. Anderson, L. A. Frank, and G. K. Parks, Upstream particles observed in the earth's foreshock region, *J. Geophys. Res., 86*, 4379, 1981.

Edmiston, J. P., C. F. Kennel, and D. Eichler, Escape of heated ions upstream of a quasiparallel shock, submitted to *J. Geophys. Res.*, 1982.

Eichler, D., Energetic particle spectra in finite shocks: The earth's bow shock, *Astrophys. J., 244*, 711, 1981.

Ellison, D. C., Monte Carlo simulation of charged particles upstream of the earth's bow shock, *Geophys. Res. Lett., 8*, 991, 1981.

field, D. H., Bow shock associated waves observed in the far upstream interplanetary medium, *J. Geophys. Res., 74*, 3541, 1969.

Fisk, L. A., Increases in the low energy cosmic ray intensity at the front of propagating interplanetary shock waves, *J. Geophys. Res., 76*, 1662, 1971.

Fisk, L. A., and M. A. Lee, Shock acceleration of energetic particles in corotating interaction regions in the solar wind, *Astrophys. J., 237*, 620, 1980.

Forman, M. A., First-order Fermi acceleration of the diffuse ion population near the earth's bow shock, *Proc. Int. Conf. Cosmic Rays 17th, 3*, 467, 1981.

Formisano, V., Low-frequency waves observed in the vicinity of the earth s bow shock, *Nuovo Cimento, 2C*, 789, 1979.

Fredericks, R. W., A model for generation of bow shock associated upstream waves, *J. Geophys. Res., 80*, 7, 1975.

Gary, S. P., J. T. Gosling, and D. W. Forslund, The electromagnetic ion beam instability upstream of the earth's bow shock, *J. Geophys. Res., 86*, 6691, 1981.

Gleeson, L. J., and W. I. Axford, Cosmic rays in the interplanetary medium, *Astrophys. J., 149*, L115, 1967.

Goldstein, B., and G. L. Siscoe, Spectra and cross spectra of solar wind parameters from Mariner 5, in *Solar Wind, NASA Spec. Publ. 308*, p. 506, 1972.

Goldstein, M. L., A non-linear theory of cosmic-ray pitch-angle diffusion in homogeneous magnetostatic turbulence, *Astrophys. J., 204*, 900, 1976.

Gosling, J. T., J. R. Asbridge, S. J. Bame, G. Paschmann, and N. Sckopke, Observations of two distinct populations of bow shock ions, *Geophys. Res. Lett., 5*, 957, 1978.

Gosling, J. T., J. R. Asbridge, S. J. Bame, W. C. Feldman, Ion acceleration at the earth's bow shock: A review of observations in the upstream region, in *Particle Acceleration Mechanisms in trophysics*, AIP Conference Proceedings, No. 56, AIP, New rk, 1979.

Greenstadt, E. W., *Phenomenology of the Earth s Bow Shock System: A Summary Description of Experimental Results, Magnetospheric Particles and Fields*, p. 13, edited by B. M. McCormac, D. Reidel, Hingham, Mass., 1976.

Greenstadt, E. W., I. M. Green, G. T. Inoye, A. J. Hundhausen, S. J. Bame, and I. B. Strong, Correlated magnetic field and plasma observations of the earth's bow shock, *J. Geophys. Res., 73*, 51, 1968.

Hoppe, M. M., C. T. Russell, L. A. Frank, T. E. Eastman, and E. W. Greenstadt, Upstream hydromagnetic waves and their association with backstreaming ion populations: ISEE 1 and 2 observations, *J. Geophys. Res., 86*, 4471, 1981.

Hudson, P. D., Reflection of charged particles by plasma shocks, *Mon. Not. R. Astron. Soc., 131*, 23, 1965.

Ipavich, F. M., G. Gloeckler, C. Y. Fan, L. A. Fisk, D. Hovestadt, B. Klecker, J. J. O'Gallagher, and M. Scholer, Initial observations of low energy charged particles near the earth's bow shock on ISEE 1, *Space Sci. Rev., 23*, 93, 1979.

Ipavich, F. M., A. B. Galvin, G. Gloeckler, M. Scholer, D. Hovestadt, and B. Klecker, Composition and energy spectra of low energy ions observed upstream of the earth's bow shock (abstract), *Eos Trans. AGU, 61*, 351, 1980.

Ipavich, F. M., A. B. Galvin, G. Gloeckler, M. Scholer, and D. Hovestadt, A statistical survey of ions observed upstream of the earth's bow shock: Energy spectra, composition, and spatial variation, *J. Geophys. Res., 86*, 4337, 1981*a*.

Ipavich, F. M., M. Scholer, and G. Gloeckler, Temporal development of composition, spectra, and anisotropies during upstream particle events, *J. Geophys. Res., 86*, 11, 153, 1981*b*.

Jokipii, J. R., Cosmic ray propagation, 1, Charged particles in a random magnetic field, *Astrophys. J., 146*, 480, 1966.

Jokipii, J. R., Propagation of cosmic rays in the solar wind, *Rev. Geophys. Space Phys., 9*, 27, 1971.

Jones, F. C., T. B. Kaiser, and T. J. Birmingham, New approach to cosmic ray diffusion theory, *Phys. Rev. Lett., 31*, 485, 1973.

Kulsrud, R., and W. P. Pearce, The effect of wave-particle interactions on the propagation of cosmic rays, *Astrophys. J., 156*, 445, 1969.

Lee, M. A., Self-consistent kinetic equations and the evolution of a relativistic plasma in an ambient magnetic field, *Plasma Phys., 13*, 1079, 1971.

Lee, M. A., Cosmic-ray evolution due to interactions with self-excited plasma waves, *Astrophys. J., 178*, 837, 1972.

Lee, M. A., and H. J. Völk, Damping and nonlinear wave-particle interactions of Alfvén waves in the solar wind, *Astrophys. Space Sci., 24*, 31, 1973.

Lee, M. A., G. Skadron, and L. A. Fisk, Acceleration of energetic ions at the earth's bow shock, *Geophys. Res. Lett., 8*, 401, 1981.

Lerche, I., Unstable magnetosonic waves in a relativistic plasma, *Astrophys. J., 147*, 689, 1967.

Lin, R. P., C. I. Meng, and K. A. Anderson, 30- to 100-keV protons upstream from the earth's bow shock, *J. Geophys. Res., 79*, 489, 1974.

Paschmann, G., N. Sckopke, J. R. Asbridge, S. J. Bame, and J. T. Gosling, Energization of solar wind ions by reflection from the earth's bow shock, *J. Geophys. Res., 85*, 4689, 1980.

Paschmann, G., N. Sckopke, S. J. Bame, J. R. Asbridge, J. T. Gosling, C. T. Russell, and E. W. Greenstadt, Association of low-frequency waves with suprathermal ions in the upstream solar wind, *Geophys. Res. Lett., 6*, 209, 1979.

Paschmann, G., N. Sckopke, I. Papamastorakis, J. R. Asbridge, S. J. Bame, and J. T. Gosling, Characteristics of reflected and diffuse ions upstream from the earth's bow shock, *J. Geophys. Res., 86*, 4355, 1981.

Russell, C. T., Comments on the measurement of power spectra of the interplanetary magnetic field in *Solar Wind, NASA Spec. Publ. 308*, p. 365, 1972.

Sanderson, T. R., R. Reinhard, and K.-P. Wenzel, The propagation of upstream protons between the earth s bow shock and ISEE 3, *J. Geophys. Res., 86*, 4425, 1981*a*.

Sanderson, T. R., V. Domingo, R. Reinhard, and K.-P. Wenzel, Anisotropy characteristics of upstream proton events, *Proc. Int. Conf. Cosmic Rays 17th, 3*, 483, 1981*b*.

Sanderson, T. R., R. Reinhard, K.-P. Wenzel, D. G. Mitchell, and E. C. Roelof, ISEE 3/IMP 8 observations of simultaneous upstream proton events, *Proc. Int. Conf. Cosmic Rays 17th, 10*, 136, 1981*c*.

Scholer, M., G. Gloeckler, F. M. Ipavich, D. Hovestadt, and B. Klecker, Pitch angle distributions of energetic protons near the earth's bow shock, *Geophys. Res. Lett., 6*, 707, 1979.

Scholer, M., F. M. Ipavich, G. Gloeckler, and D. Hovestadt, Conditions for acceleration of energetic ions ≳30 keV associated with the earth's bow shock, *J. Geophys. Res., 85*, 4602, 1980*a*.

Scholer, M., F. M. Ipavich, G. Gloeckler, D. Hovestadt, and B. Klecker, Upstream particle events close to the bow shock and 200 R_E upstream: ISEE 1 and ISEE 3 observations, *Geophys. Res. Lett.*, *7*, 73, 1980*b*.

Scholer, M., F. M. Ipavich, and G. Gloeckler, Beams of protons and alpha particles ≥30 keV/charge from the earth's bow shock, *J. Geophys. Res.*, *86*, 4374, 1981*a*.

Scholer, M., F. M. Ipavich, G. Gloeckler, and D. Hovestadt, Simultaneous observations of energetic protons close to the bow shock and far upstream, *J. Geophys.*, *49*, 186, 1981*b*.

Sentman, D. D., C. F. Kennel, and L. A. Frank, Plasma rest frame distributions of suprathermal ions in the earth's foreshock region, *J. Geophys. Res.*, *86*, 4365, 1981*a*.

Sentman, D. D., J. P. Edmiston, and L. A. Frank, Instabilities of low frequency, parallel propagating electromagnetic waves in the earth's foreshock region, *J. Geophys. Res.*, *86*, 7487, 1981*b*.

Skadron, G., and M. A. Lee, The two-dimensional structure of diffuse energetic ions associated with the earth's bow shock, Submitted to *Astrophys. J.*, 1982.

Skilling, J., Cosmic ray streaming, III, *Mon. Not. R. Astron. Soc.*, *173*, 255, 1975.

Sonnerup, B. U. Ö., Acceleration of particles reflected at a shock front, *J. Geophys. Res.*, *74*, 1301, 1969.

Stevens, G. A., and J. J. van Rooijen, The distribution function of upstream energetic particle populations, *J. Geophys. Res.*, *86*, 4435, 1981*a*.

Stevens, G. A., and J. J. van Rooijen, Directional distributions of energetic particle fluxes, *Proc. Int. Conf. Cosmic Rays 17th*, *10*, 28, 1981*b*.

Tademaru, E., Plasma instabilities of streaming cosmic rays, *Astrophys. J.*, *158*, 959, 1969.

Terasawa, T., Origin of 30–100 keV protons observed in the upstream region of the earth's bow shock, *Planet. Space Sci.*, *27*, 365, 1979.

Terasawa, T., Energy spectrum of ions accelerated through Fermi process at the terrestrial bow shock, *J. Geophys. Res.*, *86*, 7595, 1981.

Völk, H. J., Non-linear perturbation theory for cosmic ray propagation in random magnetic fields, *Astrophys. Space Sci.*, *25*, 471, 1973.

Wentzel, D. G., Hydromagnetic waves excited by slowly streaming cosmic rays, *Astrophys. J.*, *152*, 987, 1968.

(Received November 16, 1981;
revised March 18, 1982;
accepted April 5, 1982.)